Implementation of a Wireless Sensor on the Dowling Hall Footbridge for Structural Health Monitoring

A senior honors thesis

submitted by

Cynthia Lee

Bachelor of Science

in

Civil Engineering

Graduation Date: May 18, 2014

TUFTS UNIVERSITY

April 2014

Thesis Committee:
Assistant Professor Babak Moaveni
Professor Masoud Sanayei

Table of Contents

List of Figures

List of Tables

ABSTRACT

I performed this study under the supervision of Assistant Professor Babak Moaveni in order to complete the requirements for an undergraduate Senior Thesis at Tufts University. Vibration-based structural health monitoring can detect damage on a structure with the use of sensors and data acquisition systems. Previously at Tufts University, a research group implemented a wired sensing system on the Dowling Hall Footbridge to determine the dynamic parameters of the bridge. If the bridge's dynamic parameters change, it indicates a change in the bridge's structural properties, and therefore damage is detected. This research project focuses on the investigation of possible wireless sensing options for the same bridge. Sensors were compared based on specifications such as their sensitivities and noise floors. Once a sensor was chosen, it was evaluated on a shaker alongside different types of wired accelerometers. An error analysis was performed to quantify the variability of the measurements. Finally, the new wireless sensor was implemented on the Dowling Hall Footbridge to further evaluate the feasibility of an entire wireless array with it.

ACKNOWLEDGEMENTS

I completed this research with funding from the National Science Foundation (Grant No. 1125624) under the Broadening Participation Research Initiation Grants in Engineering (BRIGE) program and the John A. Cataldo Research Scholarship. I am grateful for the opportunity and funding to participate in this research as a senior undergraduate student at the Tufts University School of Engineering.

I am also grateful for the advice and support from Professor Babak Moaveni over the past year. I would like to thank Professor Masoud Sanayei as well for being a part of my thesis committee and my advisor for the past two years. You have both sparked my interest in structural engineering and teaching, and I appreciate the time you have both spent to help me learn.

Thank you to Professor Usman Khan in the electrical engineering department at Tufts University for meeting with me on several occasions. Thank you to Professor Yang Wang at the Georgia Institute of Technology and Professor Jerome Lynch at the University of Michigan for your advice and suggestions about the Narada Wireless Sensing Unit and academic solutions available. Thank you to the ever-patient support and insight from various companies: Chris Jank (PCB Piezotronics), Dr. Andy Zimmerman (Civionics, LLC), Mike Whiteman (Silicon Designs, Inc.), and Trish Nudi (MEMSIC, Inc.).

I am thankful for the entire civil and environmental engineering department – faculty, staff, and students (especially the senior class of 2014) – at Tufts University. For me, this department has become a community that I can rely on to teach me, challenge me, humble me, and best of all, make me laugh. I am thankful for the family I have with the Interdenominational Christian Fellowship (especially the senior class of 2014) at Tufts. Thank you all for your

constant friendships, wonderful personalities, and endless encouragement over the past four years. My experiences at Tufts would not have been the same without you.

Thank you to Yilan Zhang, Iman Behmanesh, Chris Paetsch, and the other graduate students who gave me advice regarding my research and future plans. Thank you to Shayne Hubbard for your impressive patience and for teaching me more about signal processing and sensors. Thank you to Yuanyuan Wang for helping me to run tests in the Structures Laboratory and for explaining various concepts to me. Thank you to Ji-Sun Ham, Timothy Peng, Kenia Estevez, Julie Doherty, Corey Diamant, Sarah Ruckhaus, and Clara Bieck for assisting me with testing on the Dowling Hall Footbridge. Thank you to Bianca Blakesley for motivating me to work on our theses together. And a special thank you to Clara Bieck, as the keeper of my sanity and best roommate I could have ever asked for. Here's to the firefly moments in the years to come! Finally, thank you to my parents and sisters for your unending, unconditional love and support throughout my life and time at Tufts University. I would not be who I am today without you.

1.0 INTRODUCTION

1.1 Aging Infrastructure and a Need for Structural Health Monitoring

The civil infrastructure in the United States is gradually aging and deteriorating. The average age of bridges in the United States is 42 years, with most bridges designed for a 50-year life span. The American Society of Civil Engineers released their latest report card for the nation's infrastructure in 2013, and the results proved dissatisfactory. The overall grade was a D+, up from a D from the previous report in 2009. The category for bridges earned a C+, up

from the C it earned in 2009, but this still leaves about 25% of the nation's bridges as structurally deficient or functionally obsolete. The Federal Highway Administration (FHWA) has calculated that more than 30% of brides in the US are over 50 years old [3].

As the ASCE Report Cards become more widely publicized, the American public has shown increasing concern for the current state of our nation's infrastructure. The latest ASCE Report Card's results were mocked on the satirical television show, The Colbert Report, on a segment in April 2013 called Tiny Triumphs. Specifically, the segment mocked the bridges section of the report card by sarcastically praising the improvements to the results from previous years while still earning mediocre or lesser grades. With this increased public awareness, there is more demand now than ever for a dedication to safety and higher standards for safety [3, 11].

Furthermore, recent technology has increased focus on predicting damage directly after a catastrophic event such as a blast or an earthquake. The ability to quantify damage that occurs to structures after a damaging event such as these can save many lives and provide information about how to design safer structures in the future.

However, as the bridges and roadways in the country have aged and changed, the methods for detecting damage and potential failures largely have not. Visual inspection is still the most common method of monitoring structures in the United States. This process is insufficient for detecting the internal damage that could exist on a structure, as the exterior of a structure could appear sound. Furthermore, visual inspections are time consuming and therefore, expensive due to the need to hire qualified inspectors and the possible need to remove non-structural elements of a structure in order to complete the inspection.

Structural health monitoring is the process for detecting damage that can occur in a building, bridge or any other structure. Historically, this has included visual inspection and other qualitative methods, but recent research in structural health monitoring is centered on quantifying damage that occurs in civil infrastructure, aerospace structures, and other industries through vibration measurements [6].

1.2 Brief Overview of Vibration Based Structural Health Monitoring

Structural health monitoring has grown significantly over the past 15 or so years and is important to evaluating and maintaining our nation's infrastructure. SHM makes use of measured acceleration, strain, and temperature at various locations on a structure. Sensors can provide real-time damage detection, which is especially important after a large-scale disaster such as an earthquake or blast [7].

Vibration-based structural health monitoring is based on the premise that the dynamic parameters of a structure are functions of its structural properties. For instance, if the natural frequencies, the dynamic parameters, of a structure change a certain amount, it indicates a change in the structure's stiffness. A change in stiffness indicates damage has occurred because stiffness is a structural property [7].

1.3 Benefits of Wireless Sensing for Vibration Based Structural Health Monitoring

The hefty cost of wired SHM systems is one of the main challenges in starting more vibration-based SHM systems on civil structures. The largest cost associated with a wired SHM

system is installation. Wired systems are also very time-consuming to install, and after a damaging event, an emergency installation of a wired system is not practical [7].

Thus, a wireless sensor system is more cost effective, and recently, wireless systems have received more and more attention in research. Two major challenges often encountered when implementing wireless sensors are long transmission ranges and battery power. The power requirement for wireless sensors makes a wireless system difficult to maintain over time.

In terms of transmission ranges, a building or smaller bridge would not typically have any issues, since a data acquisition system could be placed centrally. For a large building or bridge, range would become an issue when placing these sensors. One possible solution to this challenge is to set up multiple base stations for data acquisition on a large-scale structure. In general, wireless sensor systems need more research to see whether or not they are maintainable options for vibration-based structural health monitoring [7].

1.4 The Dowling Hall Footbridge at Tufts University

At Tufts University, the Dowling Hall Footbridge is 144 feet long and 12 feet wide. It is continuous steel frame, specifically a Warren truss. The bridge is an ideal test bed for a structural health monitoring system because it is flexible enough that an observer can feel the bridge's vibrations by simply standing on the bridge [9]. The bridge is also subjected to high volumes of pedestrian traffic daily, mostly because the university's undergraduate admissions office conducts information sessions and tours to prospective students and families from Dowling Hall.

Dowling Hall is also home to Tufts' Student Services, Financial Aid, Career Services, and other offices that increase pedestrian traffic across the bridge.

The bridge is supported at three locations: one end is supported at an abutment facing the academic quad, the other is supported a pier next to Dowling Hall and a third support is located at mid-span. Previously in 2009 and 2012, components for a wired SHM system were installed on the bridge. This system provided ambient vibration data for estimating the modal parameters of the bridge every hour. Previous students – Peter Moser, Alyssa Kody (E13), Xiang Li, and Iman Behmanesh – in Professor Moaveni's research group have worked on the installation and evaluation of this wired system since 2009 [8,9].

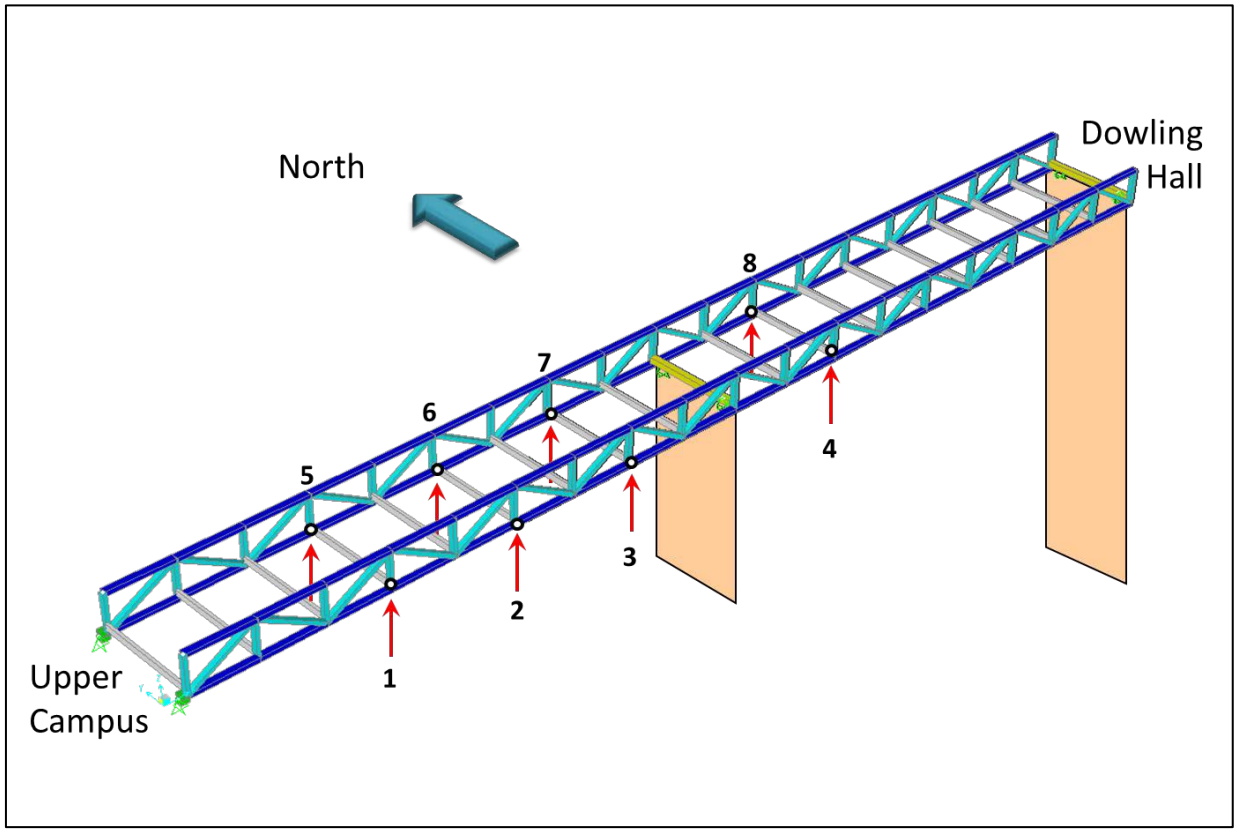

Figure 1: Model of the Dowling Hall Footbridge (Including Layout of Wired Accelerometers) [8]

From their previous research, they found that the first six natural frequencies are as follows: 4.68 Hz, 5.99 Hz, 7.16 Hz, 8.93 Hz, 13.18 Hz, and 13.71 Hz.

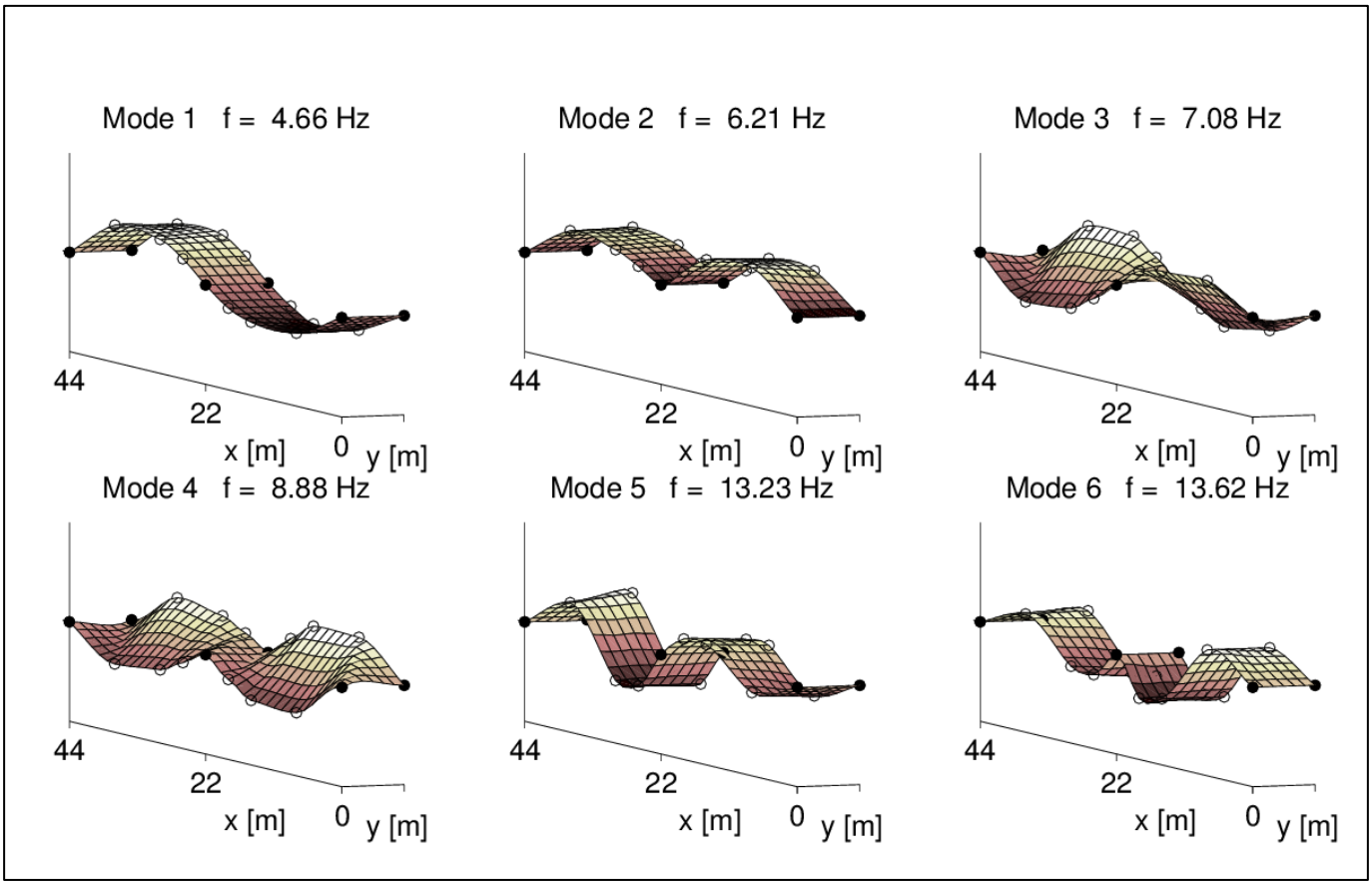

Figure 2: Natural Frequencies and Mode Shapes (Geometric Plot) of the Dowling Hall Footbridge [8]

For my research project, I investigated a wireless sensor to evaluate its performance against the current wired sensors on the bridge. For an initial wireless sensor, I looked for an accelerometer. I planned to analyze the practicality of implementing a wireless structural health monitoring system on a bridge such as the Dowling Hall Footbridge and to address the challenges associated with such a wireless system.

1.5 Selection of the Wireless Node

I first searched for commercially available wireless accelerometers. The accelerometers needed to fit several requirements. In order to be suitable for a SHM on the Dowling Hall Footbridge, they needed a high sensitivity and resolution of at least 16-bits. I also looked only for smart sensors, or sensors with an on-board CPU (central processing unit) that would allow us to program sampling rates for the sensor and give us more control over what the sensor measured. Finally, I looked for sensors with low noise floors.

My initial search revealed that only a limited number of wireless accelerometers are available commercially, and I did not find any that fit the requirements I set with Professor Moaveni for this project. I browsed options from the companies BeanAir and Monnit, both of which provide solutions for wireless structural health monitoring. These companies both provide wireless accelerometers that are geared towards structural health monitoring, but their specifications did not meet the sensitivities or other requirements we were looking for. Many other wireless sensing systems available are not intended for measuring seismic vibrations. MEMSIC, a company based in Andover, Massachusetts, previously had a wireless sensing board that included an accelerometer and temperature gauge. That wireless sensing board, the ISM400, was based on a platform called the Imote2. The Imote2 is now obsolete and its replacement, Lotus, supports a new board called the MTS400. Although this board includes an accelerometer, its main uses are for environmental sensing, and I did not consider it further for this research project.

Next, I looked into various academic solutions available and found the Narada Wireless Sensing Unit (WSU) from Civionics, LLC. The Narada WSU is a wireless node that can attach

to various types of sensors. The WSU has a 16-bit resolution and the ability to program sampling rates. It communicates with a base station that connects to a PC through a USB port. The Narada WSU provides more options for transducers in a wireless structural health monitoring system.

Unfortunately, the Narada WSU is also almost ten years old and no longer fully supported by Civionics, LLC. In search of a more recent sensor, I spoke to Professor Yang Wang from the Georgia Institute of Technology, who developed a wireless sensor board called Martlet. According to Professor Wang, the Martlet has an 80 MHz processor, which is ten times that of the Narada. The Marlet was released in the spring of 2014, which did not fit the timeline of this project. Ultimately, based on my investigation and advice from professors, I chose to purchase and evaluate the Narada WSU. The current wired accelerometers on the Dowling Hall Footbridge are from PCB Piezotronics (High Sensitivity ICP 393B04) are not compatible for the Narada WSU because the excitation voltage of the 393B04 exceeds the limits of the WSU. In order to use those accelerometers with the Narada WSU, we needed a custom signal conditioning module. Civionics provides a signal conditioning module compatible to the MEMSIC accelerometer. Therefore, I needed to search for accelerometer options compatible to the WSU.

Figure 3: Narada WSU

Figure 4: Narada Base Station

1.6 Selection of Accelerometer Compatible with Narada Node

The Narada WSU expects a voltage input of 5V, so the excitation voltage of the accelerometer should not exceed 5V. Knowing this, I narrowed the options down to three different accelerometers from three separate companies. The first was a triaxial accelerometer from MEMSIC (TG-Series 3-Axis), the second option was a single axis accelerometer from Silicon Designs (2012-002), and finally, I considered the T0-8 embeddable accelerometer from PCB Piezotronics. Support at PCB Piezotronics suggested using the T0-8 low cost, embeddable accelerometer with the Narada WSU, and I hoped that these would be comparable to the 393B04. However, this accelerometer is also not intended for seismic vibration measurements and is instead intended for original equipment manufacturer applications.

In terms of cost, the MEMSIC accelerometer was most expensive, at $1295, before shipping and taxes. The Silicon Designs accelerometer cost $435, and the PCB T0-8 cost $155.

I also directly compared the frequency ranges – that is, the frequencies that the accelerometer can measure – of the three accelerometers. The ranges were as follows: 0-300 Hz for the Silicon Designs 2012-002, >200 Hz for the MEMSIC TG-Series, and 0.32-8000 Hz for the PCB T0-8.

Lastly, I compared the sensitivities and excitation voltages for the accelerometers. These were 1000 mV/g and 4.75 to 5.25 V, 833 mV/g and 3.3 to 5.5 V, and 1000 mV/g and 3 to 12 V for the Silicon Designs, MEMSIC, and PCB accelerometers, respectively. After comparing these factors, I decided to use the Silicon Designs 2012-002 with the Narada WSU. I decided to use the 2012-002 mainly because it does not require a signal conditioner and because its frequency range begins at 0 Hz [1, 2].

Figure 5: Example Silicon Designs Sensor

Figure 6: PCB T0-8

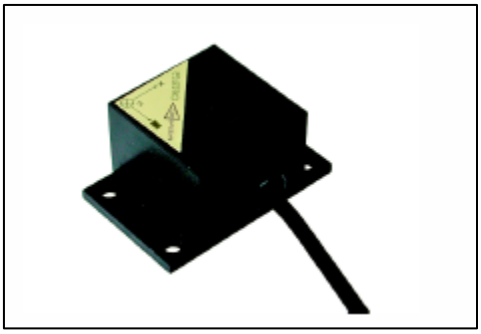

Figure 7: Example MEMSIC Sensor

1.7 Setup of the Narada WSU and Base Station

After purchasing the Narada Wireless Sensing Unit and Base Station, I downloaded and installed the Narada Executable. Civionics provided operating instructions for setting up the WSU and beginning data acquisition with the executable. Civionics also provided a Matlab code to plot the acquired data on a Voltage Versus Time graph. I installed the executable on a PC in Anderson 206A with the help of the Tufts Information Technology Office, and began to familiarize myself with the program. The Narada Executable is downloaded with two files that can be saved and configured in any word editor: the default_settings.dat file and the DAQ_settings.dat file. The DAQ settings file allows the user to program different sampling rates and test times, and the default settings file controls the network settings (i.e. channel changes for less interference) for the system [5].

Next, I connected the Silicon Designs 2012-002 to the WSU. The WSU has four channels to which a transducer can be attached. I attached the 9V battery pack (6 AA batteries) to the two pins at the top of the WSU first and checked that the WSU turned on correctly. With the help of students in the Electrical Engineering department at Tufts University, I checked that the correct pins for each of the channels read 5V when the WSU was on.

The 2012-002 has four wires (green, black, red, and white) that connect it to a data acquisition system, or in this case, the Narada WSU. I purchased Molex parts to connect the accelerometer to one of the WSU channels by crimping the wires to Molex connectors that fit into the Molex housing. I covered the remaining exposed wires with heat shrink. For connection to the WSU, I followed the 2012-002 instructions for connection in single-ended use and therefore left the white wire unattached and covered it with heat shrink.

Figure 8: Molex Connector Parts
(http://media.digikey.com/photos/Molex/22-01-3037.jpg;
http://media.digikey.com/photos/Molex/08-65-0805.JPG)

Once I plugged the base station into a computer and turned on the WSU, the main commands I needed in the executable were 01: Check status of one sensor and 10: Collect DAQ data. In my initial tests of the sensor, the accelerometer sat face up on my desk, and I tapped the desk several times (the test ran for 30 seconds at a sampling frequency of 1000 Hz). During these initial tests, the acquired signals were very noisy because I had difficulties with the connection between the accelerometer and WSU, so I made adjustments over several trials. When I was confident that the connection was sound, I placed the accelerometer on top of my PC, whose fan vibrates at a frequency of 120 Hz. For this, I used a sampling frequency of 512 Hz. Through these test runs, I learned more and more about how the wireless sensor would work and found that running the test for too long would slow down data acquisition. I also found that having a sampling rate over 600 Hz would slow down data acquisition.

At this point, I wrote a new Matlab code to include a conversion from voltage into acceleration and a Fast Fourier Transform analysis. The Narada WSU reports data as an array of integers. Civionics provides the equation to convert the integers into voltage, shown below:

$$Voltage\ (V) = 5.0 * \frac{IntegerValue}{65535}$$

I then converted this voltage into acceleration using the calibration factors of the specific 2012-002 purchased (1000 mV/g). My code also normalized using the zero-g voltage of the 2012-002 provided by Silicon Designs. (Appendix A). When I ran the acquired signals through the FFT code, the data showed that the accelerometer was able to measure the 120 Hz frequency of the PC fan.

Simultaneously, I looked into weatherproof containers for the sensor when it is implemented on the Dowling Hall Footbridge. For this, a graduate student at the University of Michigan, Yilan Zhang, suggested looking for a PVC fitting. Her previous research involved the Narada WSU connected to the same MEMSIC accelerometer I looked into. She purchased PVC boxes from McMaster for her research, and I found a similar fitting from Thomas and Betts. The box was 8”x8”x6” and has a removable lid. I tested the sensor briefly inside the box to make sure that the base station recognized the signal. For test on the shaker, I planned to use wall tack to attach the sensor and all of its components to the inside of the fitting. In order to evaluate the performance of the sensor in comparison to the wired accelerometers at Tufts University, I ran several shaker tests, with the Narada sensor in and out of the box.

1.8 Performance Evaluation of the WSU

In order to evaluate the performance of the Narada WSU and Silicon Designs accelerometer before placing it on the Dowling Hall Footbridge, I tested the sensor node in the Structures Laboratory at Tufts University Civil and Environmental Engineering Department. To conduct the test, Yuanyuan Wang (E14) helped me to run the shaker in the lab. During the tests, we evaluated the Narada WSU alongside the accelerometers currently owned at Tufts University. These include the wired PCB Piezotronics accelerometers (393B04), and an accelerometer from B&K. Again, these PCB accelerometers are currently installed on the Dowling Hall Footbridge. Throughout these tests, we also had three different data acquisition (DAQ) systems. The Narada Base Station with the Narada Executable, which I ran on a PC in Anderson 206A and on a laptop that Professor Moaveni provided. The other two systems were National Instruments DAQ systems, one called cDAQ and the other, USB 6251. Both the cDAQ and USB6251 use LabView Signal Express to collect data. The cDAQ requires a sampling frequency of at least 1652 Hz, and so I used a sampling rate of 2048 for that system. For the other two systems, I used 512 Hz for the sampling rate. To run a test, first we began data collection on the cDAQ system, which we set to run continuously. Next, we began data collection on the Narada executable, and finally, we started the input signal and USB 6251 together. I programmed the Narada sensor to collect data for 60 seconds. The figures below show the general setup of each test, although the layout of the wired accelerometers varies slightly between the tests.

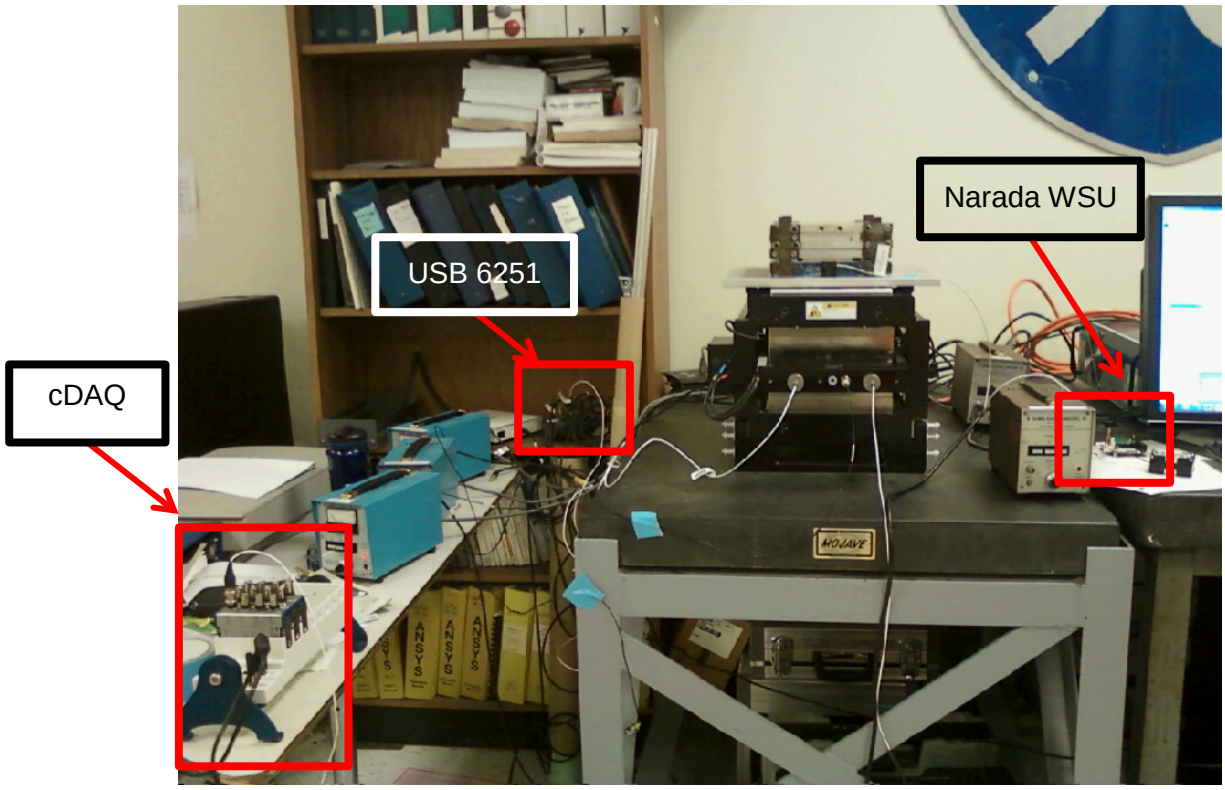

Figure 9: Setup of a Shaker Test

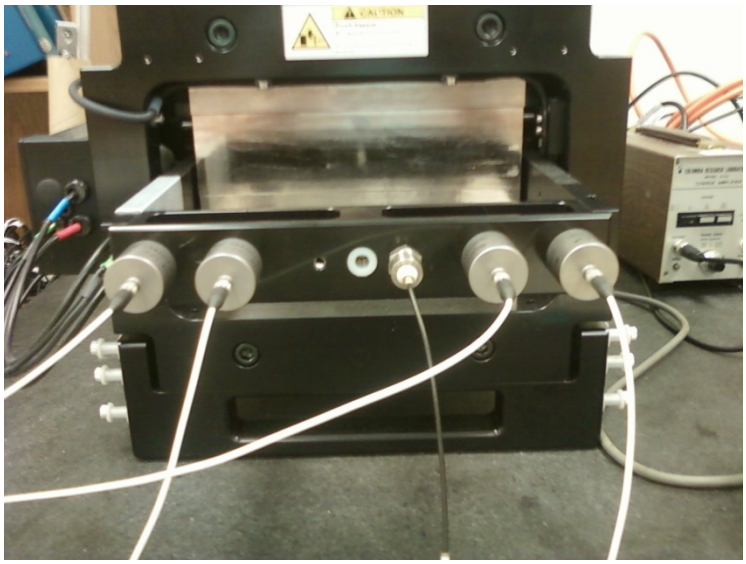

Figure 10: Front of the Shaker, 5 Wired Accelerometers Mounted

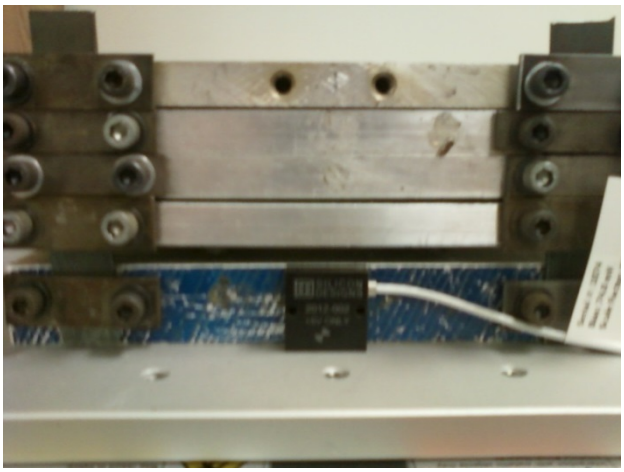

Figure 11: Silicon Designs 2012-002 Mounted to Top of Shaker

First we ran a linear sine sweep test. For this test, we attached one 393B04 to the cDAQ and another to the USB 6251 along with the B&K accelerometer. I screwed these wired accelerometers to the front of the shaker, but I had to wax the Silicon Designs accelerometer to the shaker. The Narada WSU sat on the desk, to the side of the shaker. After a few trials with this setup, we noticed a phase shift in the signals collected from the USB 6251 and unusually noisy signals from the cDAQ. These signals were also difficult to compare since there were no distinct frequencies to compare; thus, these results are not displayed here, and we prepared a second test.

For the second test, we instead ran a step sine test, with an input signal of sine waves at 2, 4, and 10 Hz, at amplitudes of 0.1, 0.5, and 1.0, respectively. Each signal was 10 seconds long. The equations for the input signals were

$$Input = 0.1\sin\left(2\pi(2\ Hz)t(1{:}500)\right)$$

$$Input(501{:}1000) = 0.5\sin(2\pi(4\ Hz)t\left(1{:}\frac{10}{0.02}\right))$$

$$Input(1001{:}1500) = \sin(2\pi(10\ Hz)t\left(1{:}\frac{10}{0.02}\right))$$

Where t = 0.02:0.02:30 seconds. Figure 5 shows the Matlab plot of the input signal.

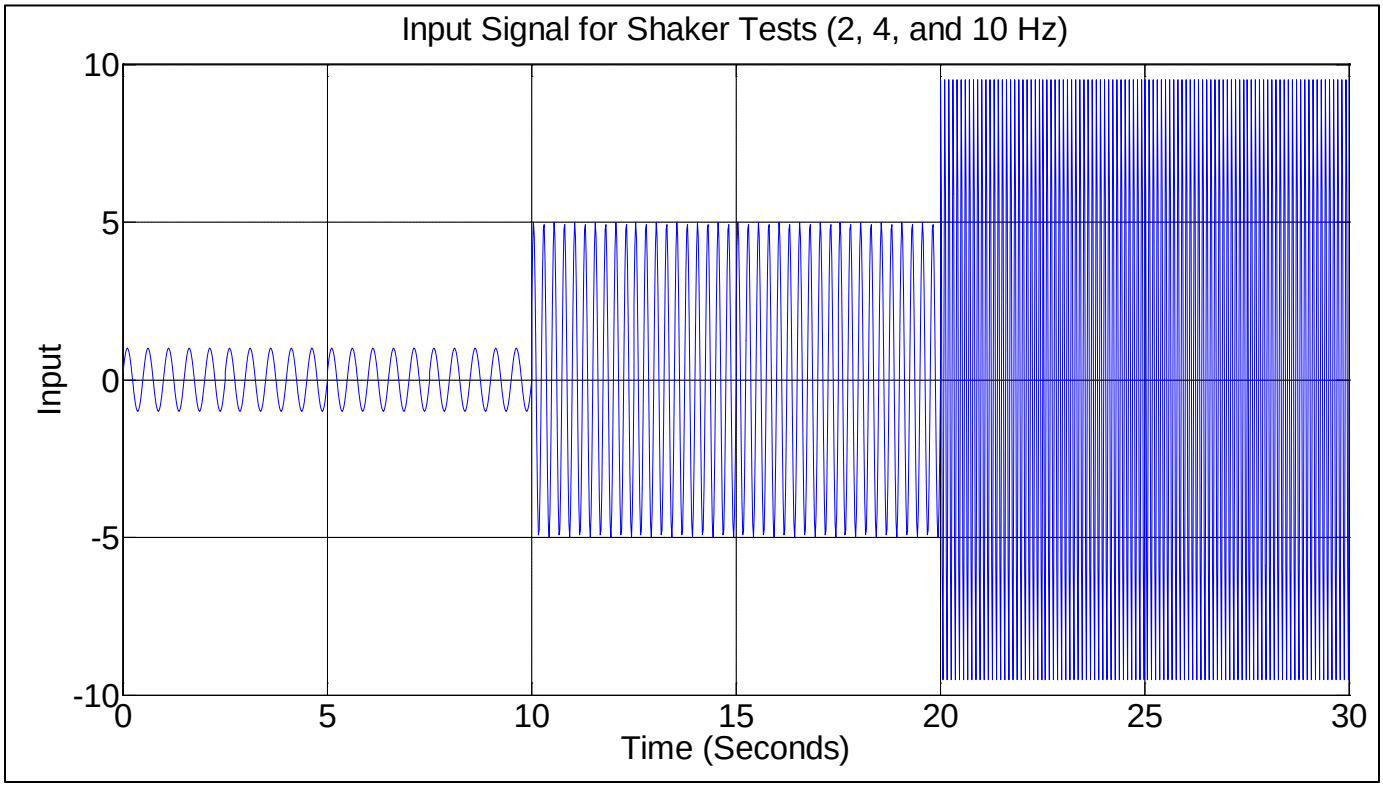

Figure 12: Plot of Input Signal

This time, we had two 393B04 accelerometers attached to each National Instruments DAQ system and the B&K accelerometer still attached to the USB 6251. Below is a list of the accelerometers for this test.

Table 1: List of Accelerometers for Shaker Test

Accelerometer	Calibration Factor
PCB 393B04 25397	1059 mV/g

PCB 393B04 25398	1055 mV/g
PCB 393B04 25401	1050 mV/g
PCB 393B04 25402	984 mV/g
B&K	349 mV/g
Narada WSU/2012-002 Sensor	1000 mV/g

An initial look at the collected signals showed that the cDAQ system was still collecting noisy signals, so we began adjusting the settings in LabView. After changing the Iex setting from “None” to “Internal,” the cDAQ collected expected signals with distinct sine waves. The signals on the USB 6251 still had shifts between them, which was unexpected given that they all began collecting data at the same time.

While we did our best to start the DAQ systems at comparable times, I performed synchronized the signals in Matlab after the tests were completed. Also in this code, I added filters to remove some lower frequencies and reduce noise.

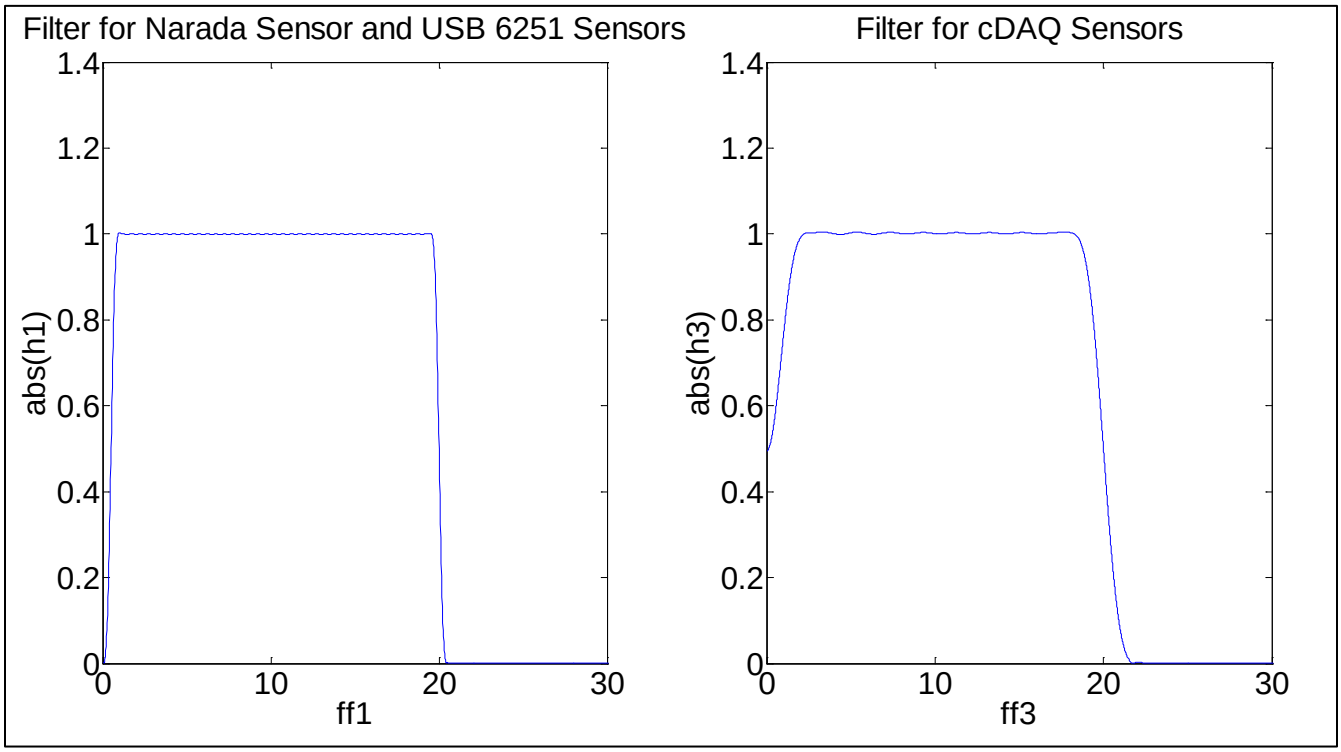

Figure 13: Plot of Filters Used in Matlab Analysis

With the signals matched on the same timeline, I again ran the filtered signals through the Fast Fourier Transform and checked that the frequencies measured were the expected 2, 4, and 10 Hz. Once synchronized, the signals showed the same frequencies, but varying magnitudes.

The figure below shows a trial from this second test, where “Narada” denotes the signal from the Narada sensor, “B&K” denotes the B&K accelerometer, “PCB 1” denotes the 393B04 25397 on the USB 6251 DAQ system, and “PCB 3” denotes the 393B04 25401 on the cDAQ system.

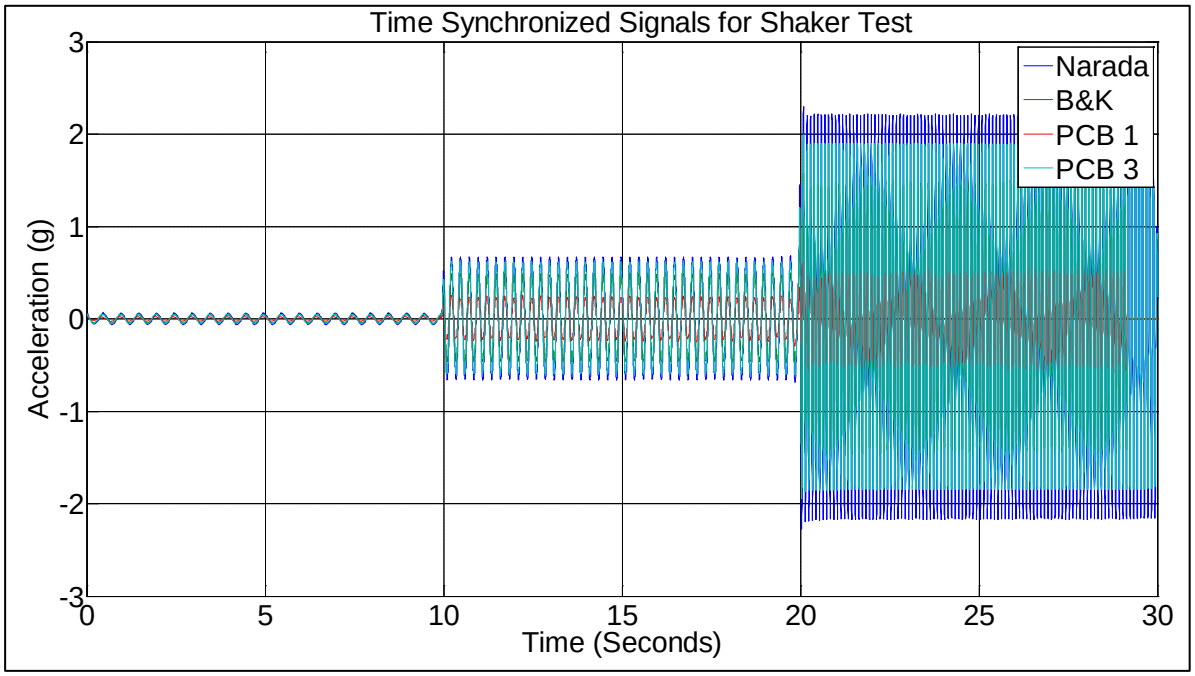

Figure 14: Plot from Shaker Test 2

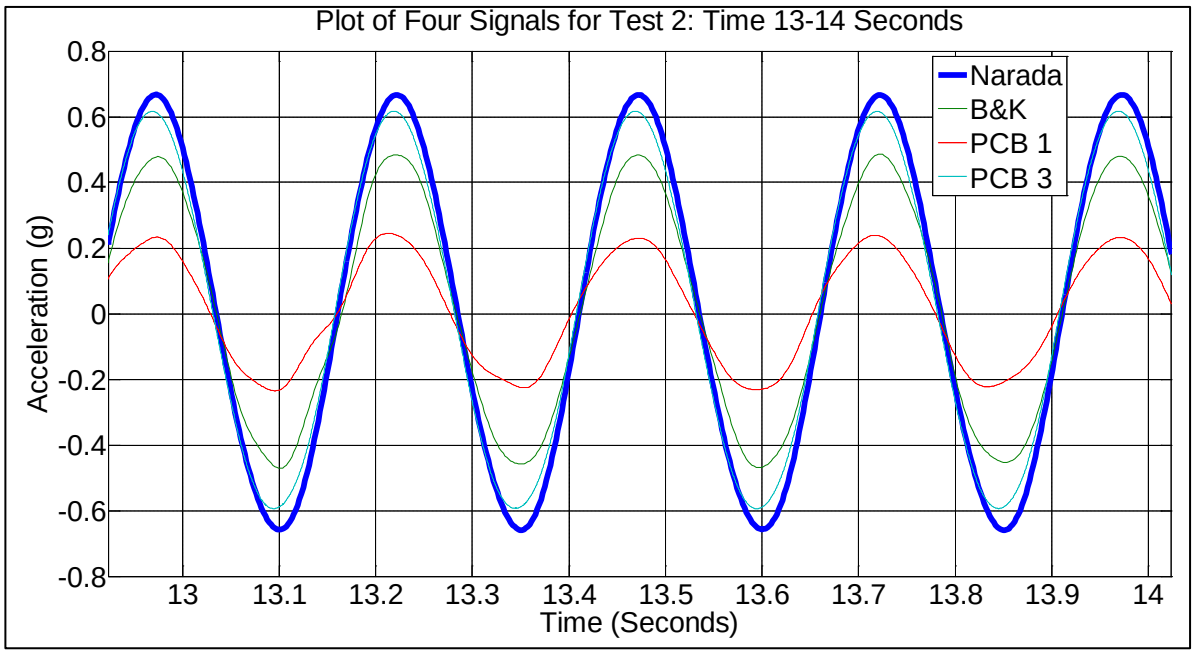

Figure 15: Close-up of Figure 14

Figure 16 below shows signals each DAQ system in the frequency domain.

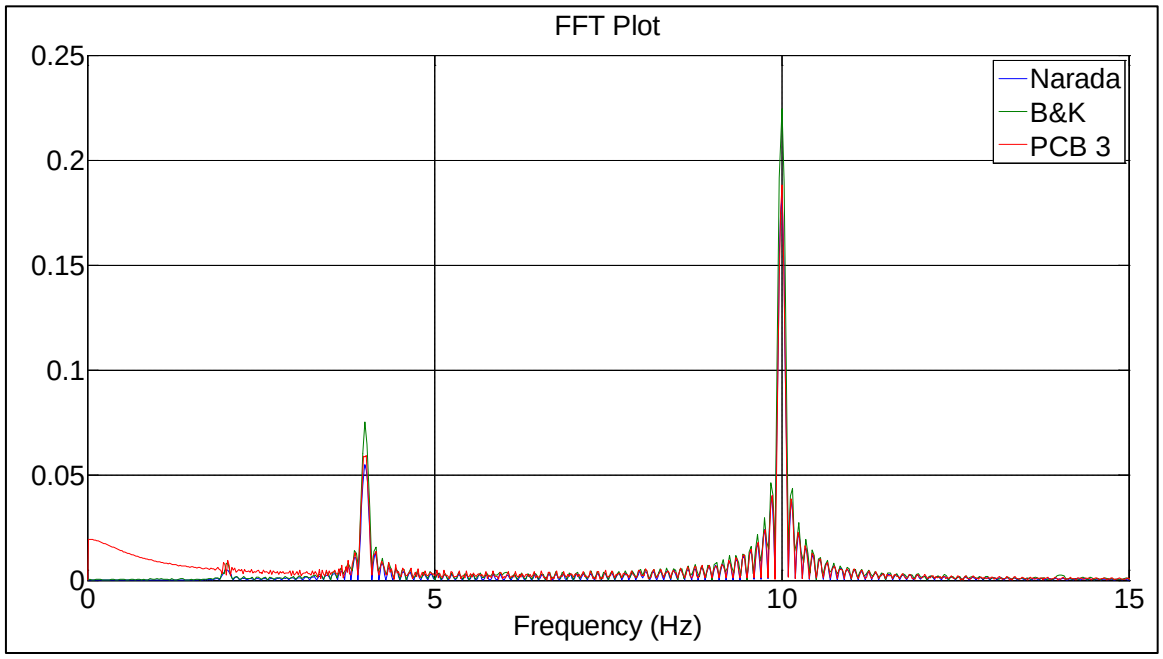

Figure 16: FFT Plot from Shaker Test 2

For the third test, we connected the B&K accelerometer to the cDAQ system and used the same input signal as in the second test. Otherwise, we also used the same six accelerometers and setup as in the second test. When connected to the cDAQ system, the B&K accelerometer was much more comparable to the Narada sensor than before. Also during the third test, we conducted three trials with the Narada sensor set up inside the PVC fitting. For this, the entire Narada sensor (accelerometer, WSU, and battery pack) were inside the fitting which we attached to the shaker with wall tack. I used the same Matlab code I previously wrote for the second test in order to analyze the data from this test. The fitting did not significantly affect the collected signals.

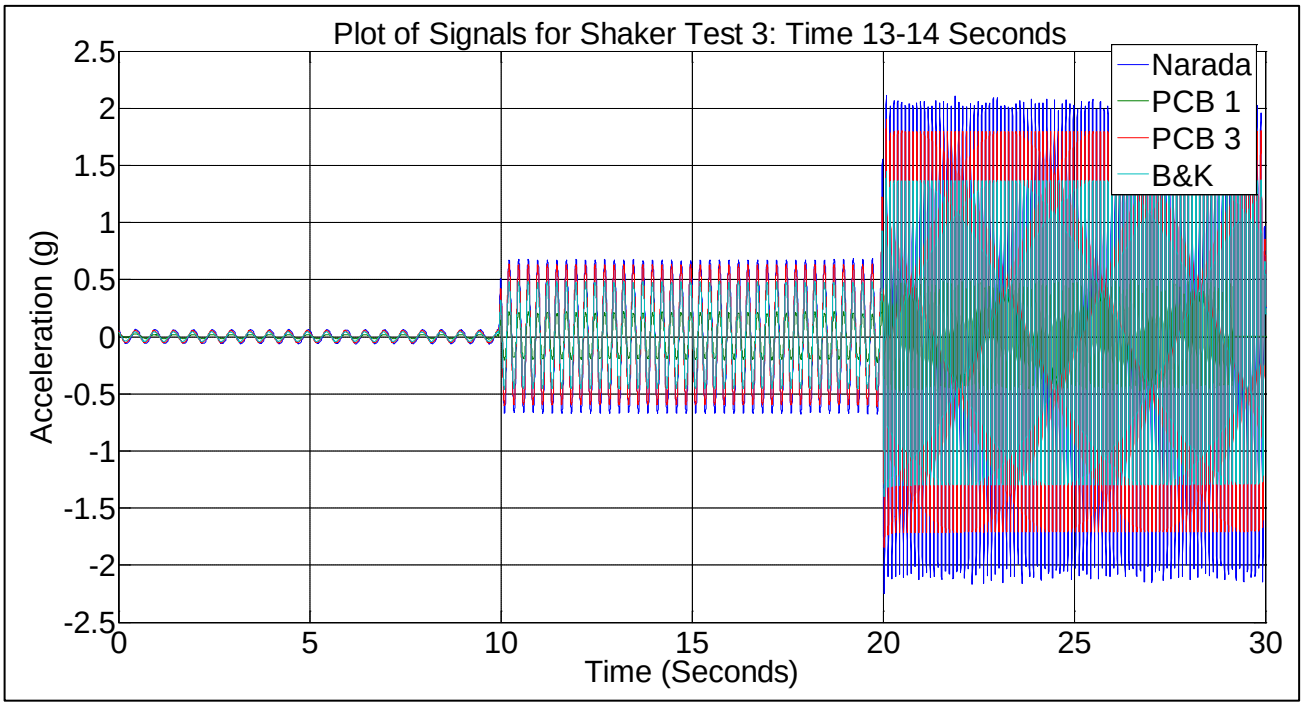

Figure 17: Plot from Shaker Test 3, Trial with Narada Sensor Inside PVC Fitting

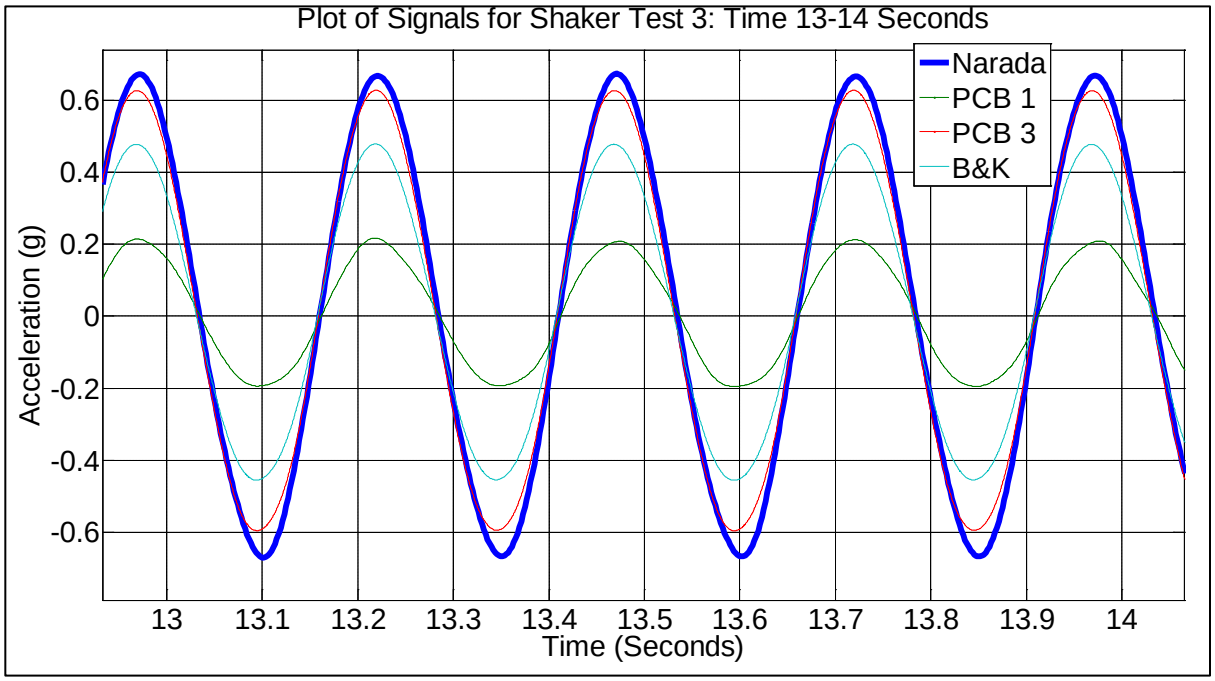

Figure 18: Close-up of Figure 17

For Figure 19, “Narada” represents the Narada sensor. “PCB 3” and “B&K” represent the PCB and BNK accelerometers on the cDAQ respectively, and “PCB 1” represents the PCB accelerometer on the USB 6251.

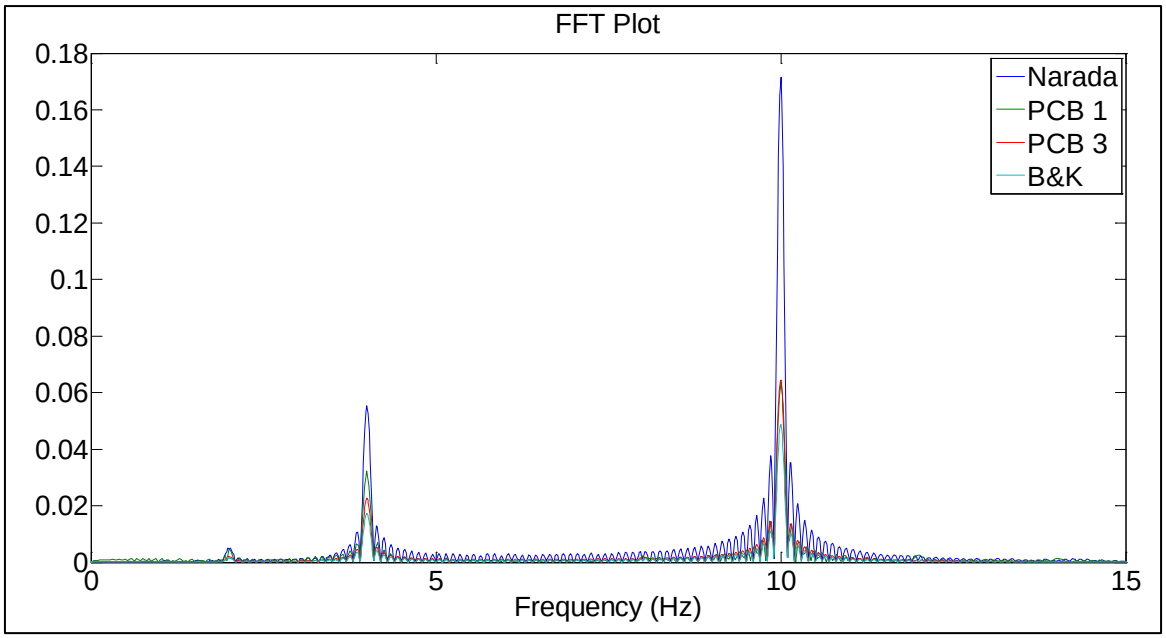

Figure 19: FFT Plot from Shaker Test 3

The signals all matched in frequency (See Figure 19) but not in magnitude, so I performed an error analysis to compare the Narada sensor’s acceleration measurements to each other accelerometer individually. I used the following equations for this error analysis:

$$E = x_1 - x_2, \;\; Percent\ Error = \frac{E'E}{x_1{}'x_1} * 100\%$$

Where x_2 represents the signal from the Narada sensor, and x_1 represents any wired accelerometer.

From this analysis, I found that when compared to wired accelerometers on the cDAQ system, the Narada sensor signal had errors of less than 10%. I could not compare the Narada

sensor to sensors on the USB 6251 given large difference in magnitudes. To calculate these errors, I compared the Narada sensor to the wired signals for each 10-second period. A more comprehensive lists of the errors I calculated from two trials are shown below.

Table 2: Percent Errors, Corresponding to Figure 8

Narada Sensor Compared to:	Percent Error
PCB1 (0-10 seconds)	558%
PCB3 (0-10 seconds)	2.21%
BNK (0-10 seconds)	9.31%
PCB1 (10-20 seconds)	491.5%
PCB3 (10-20 seconds)	0.272%
BNK (10-20 seconds)	4.48%
PCB1 (20-30 seconds)	1413%
PCB3 (20-30 seconds)	1.18%
BNK (20-30 seconds)	7.92%

The following figures show the same signals as in Figure 17, but with the signal magnitudes scaled to comparable values. These further show that the frequencies of the signals match well.

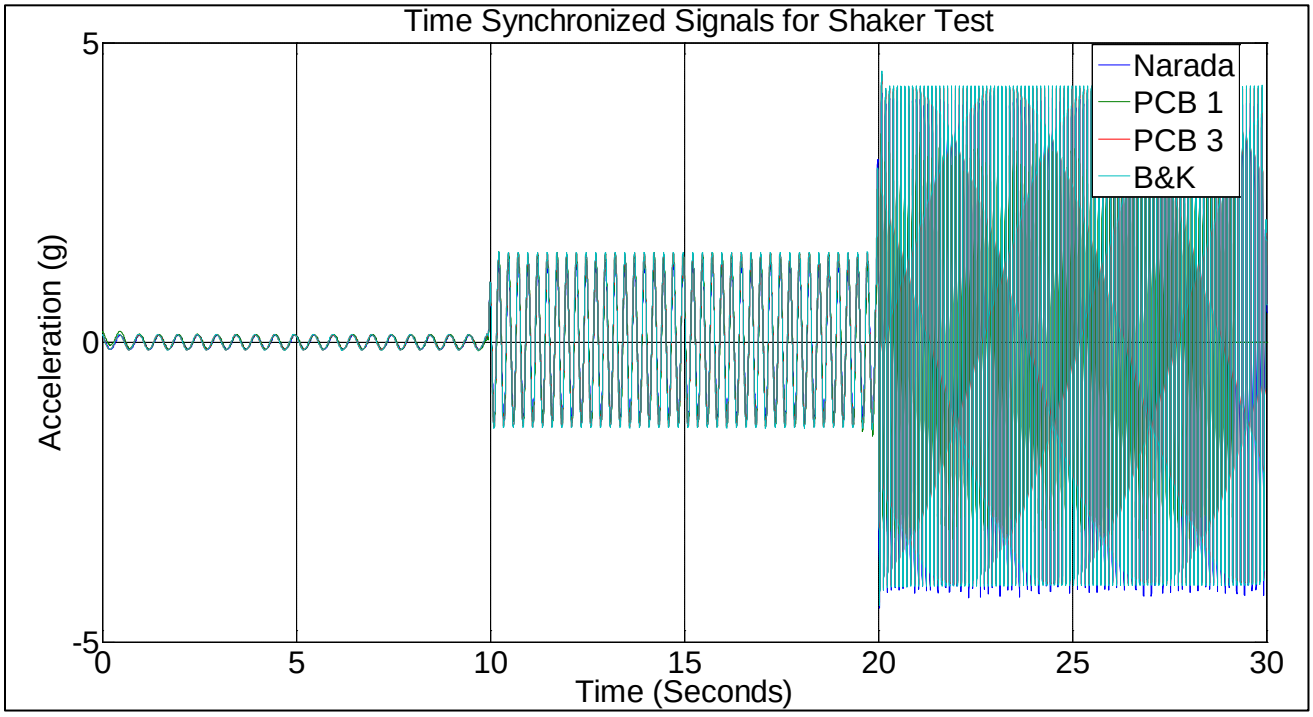

Figure 20: Plot from Shaker Test 3 with Signals Scaled to Match in Magnitude

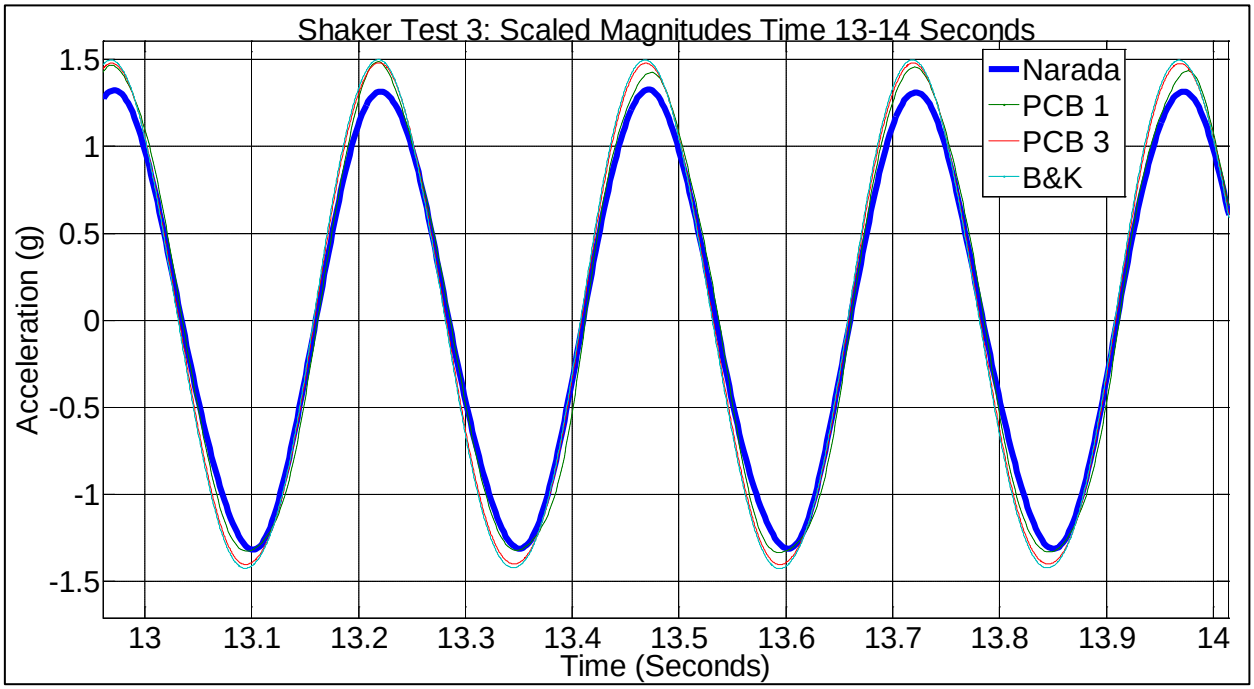

Figure 21: Close-up of Figure 20

In summary, these shaker tests showed me that the Narada sensor is comparable to the PCB accelerometers we currently have on the Dowling Hall Footbridge. The differences in magnitude from the accelerometers on the cDAQ and the Narada sensor could have been due to incorrect calibration factors. Some of the wired accelerometers have not been calibrated for several years. The accelerometers on the USB 6251 resulted in signals with much lower magnitudes than the rest, which may be a result of the aging DAQ system. Therefore, I did not use the results from the USB 6251 to evaluate the performance of the Narada sensor. These tests confirmed that the Narada sensor can be a viable option for a wireless sensor array on a small scale structure such as the Dowling Hall Footbridge, and my next steps were to test one Narada sensor on the bridge.

2.0 IMPLEMENTATION OF THE NARADA NODE ON THE DOWLING HALL FOOTBRIDGE

2.1 Setup and Data Acquisition Settings

For each of the bridge tests I conducted, the entire Narada sensor was securely attached to the inside of the PVC fitting with wall tack. I placed the PVC fitting at various locations on top of the bridge, which I have detailed in the following sections of this paper. For tests that included wired accelerometers, I used an extension cord provided by Professor Sanayei in order to use the cDAQ system. To collect data, I used a laptop provided by Professor Moaveni, which already had LabView Signal Express and on which I installed the Narada Executable. To be consistent with the preceding shaker tests, I used a sampling rate of 512 Hz for the Narada sensor and 2048 Hz for the cDAQ. For each test, I started data collection for the cDAQ system first before starting data acquisition for the Narada Executable. On the bridge, I had a few friends jump after I began both DAQ systems, so that I could synchronize the times of the signals later in Matlab. I made sure the weather was suitable for each test before setting up (i.e. no rain).

2.2 Test 1: Narada Node Test

For Test 1, I brought only the Narada node to the Dowling Hall Footbridge. I programmed the sensor to run for 60 seconds and placed the sensor at various locations on the bridge for different trials. For trials one and two, the sensor sat in the middle of the span on the campus side of the bridge. The sensor sat on the north side of the bridge. For trials three and four, I moved the sensor to the south side of the bridge. For trials five and six, I kept the sensor on the south side of the bridge and moved it to the middle of the Dowling Hall side span. (See Figure 1 for reference on these locations) The figure below shows the setup of the sensor from Trial 4.

Figure 22: Setup on the Footbridge

Figure 23: Inside the PVC Fitting

For each trial, I had a few friends jump four 5 second increments throughout the test (not including the initial jump needed to synchronize the data). They moved their jump location for

each trial, although they kept at least 5-feet away from the sensor for each trial. In Matlab, I used filters similar to the ones I used for the shaker tests for my analysis. Pictured below is the resulting filtered signal from Trial 4, during which the jumps occurred on the Dowling Hall side of the span.

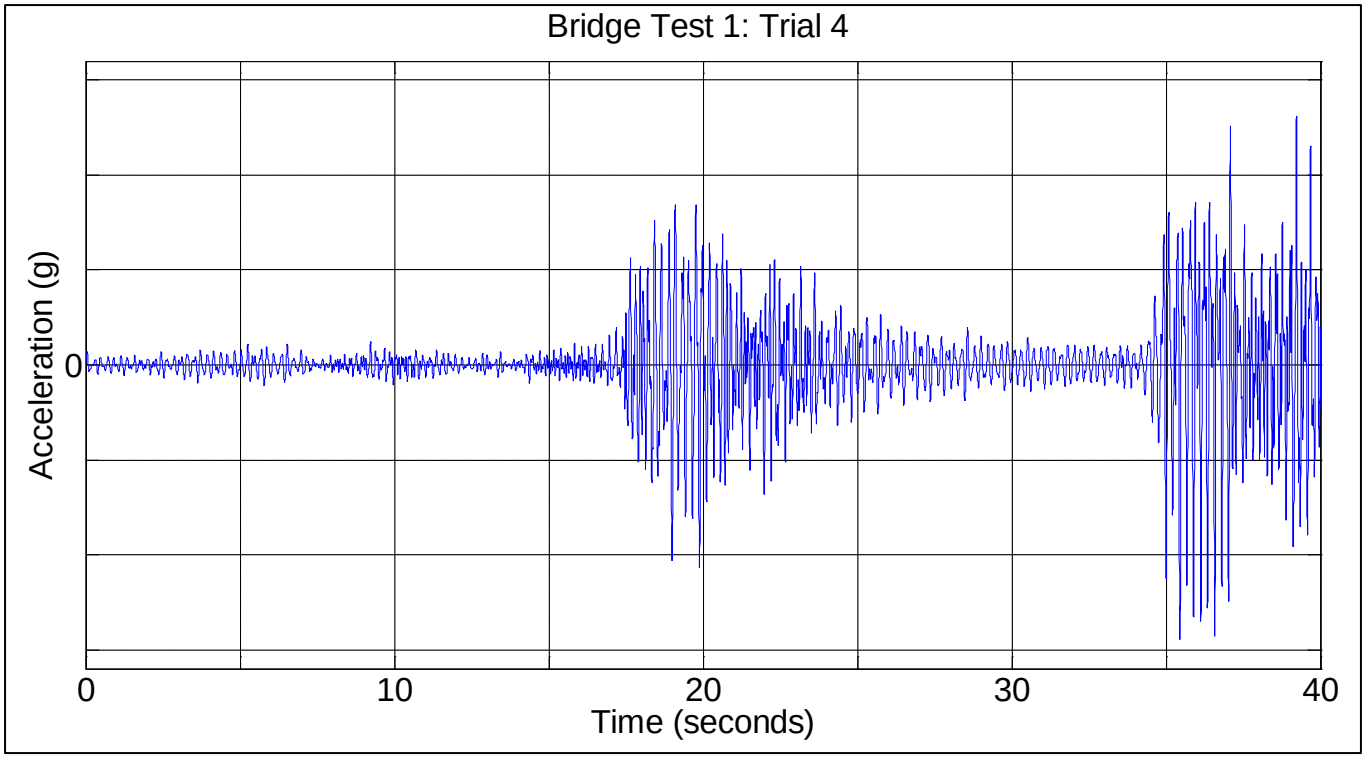

Figure 24: Filtered Signal from Trial 4

The figures below show the frequency plots of the filtered signals for Trials 1, 4, and 5:

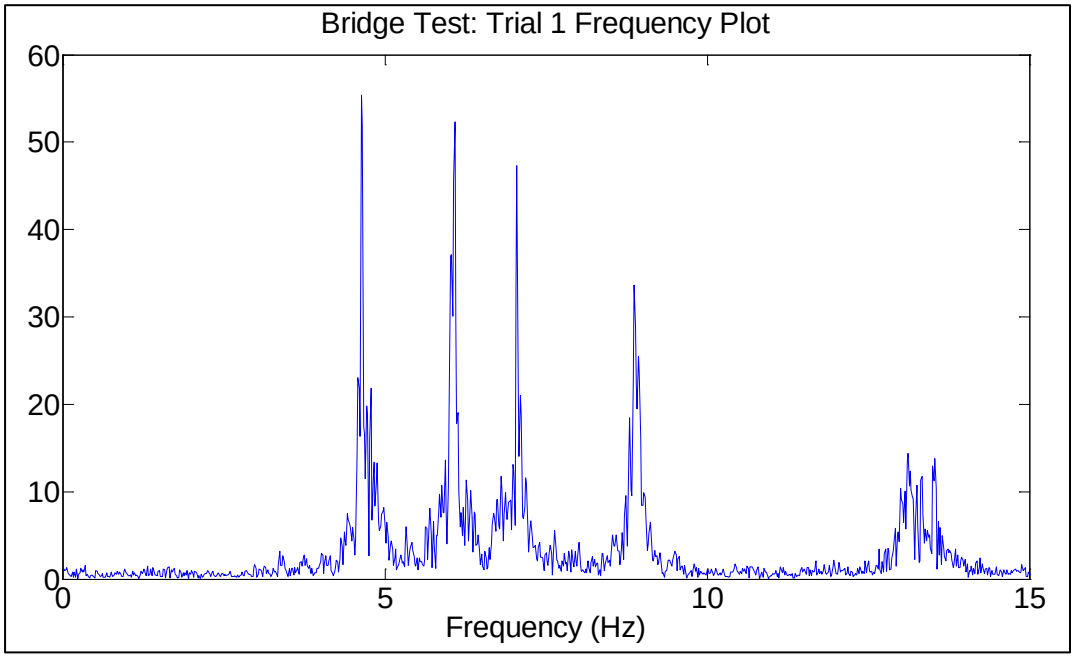

Figure 25: FFT Plot from Test 1, Trial 1

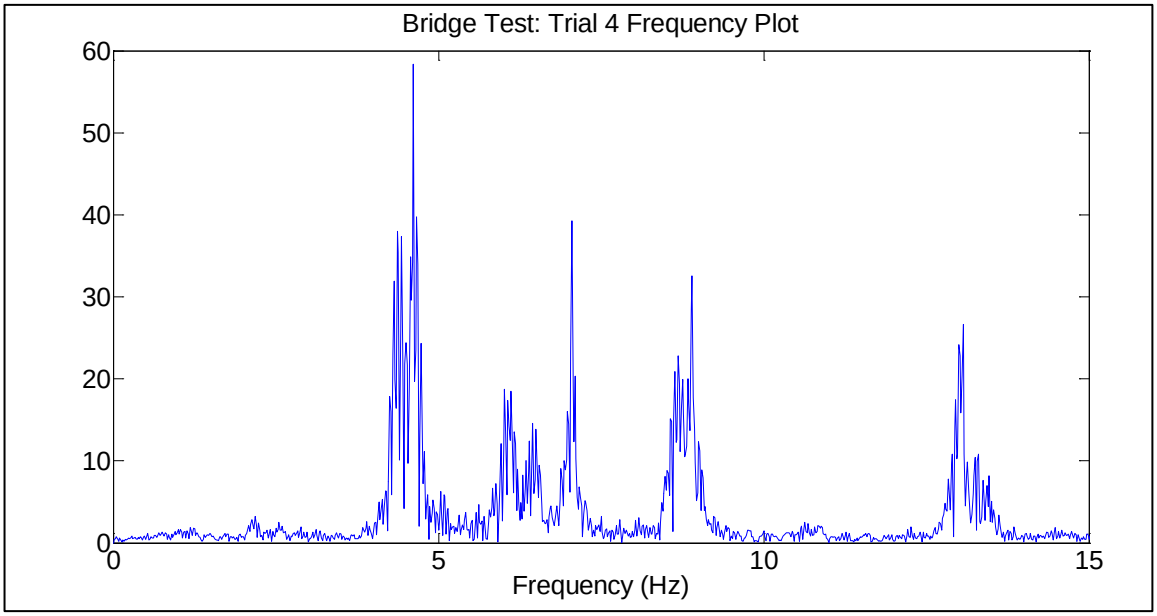

Figure 26 : FFT Plot from Test 1, Trial 4

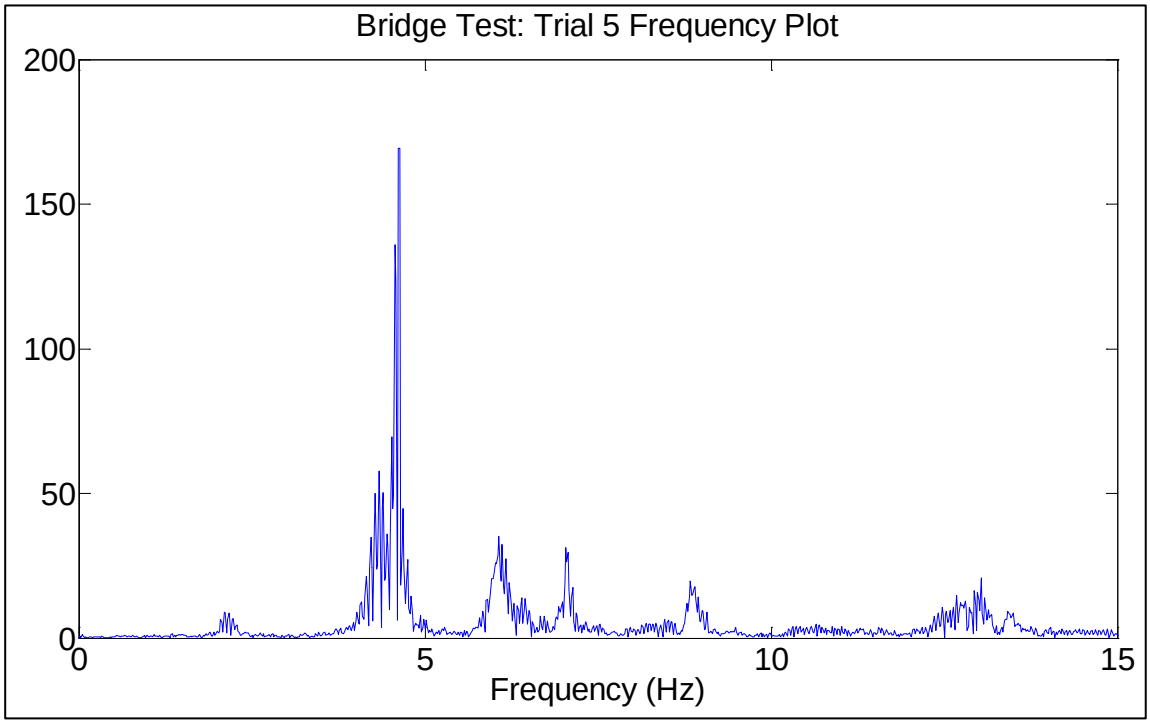

Figure 27 : FFT Plot from Test 1, Trial 5

These frequency plots show that the Narada node was consistently measuring similar natural frequencies for the bridge. A more detailed data analysis showed that the average first natural frequency measured during this test was 4.618 which has a 1.32% error when compared to the first natural frequency Moser calculated. After this initial bridge test, I planned to bring the PCB 393B04 accelerometers to the bridge to collect data simultaneously.

2.3 Test 2: Narada Node Test Alongside PCB 393B04's

In Test 2, I tested the Narada sensor on the footbridge again alongside two PCB 393B04 accelerometers. Here I tested the sensors in the middle of the academic quad side span of the bridge. The Narada sensor sat on the north side of the bridge and the PCB accelerometers sat directly across from the Narada sensor on the south side of the bridge. Again, I used a laptop to

collect signals from all three accelerometers with the Narada Executable and LabView Signal Express. The PCB accelerometers I used are as follows:

Table 3: PCB Accelerometers on the Footbridge for Bridge Test 2

PCB 393B04 25401	1050 mV/g
PCB 393B04 25402	984 mV/g

The figures below show the setup for this test.

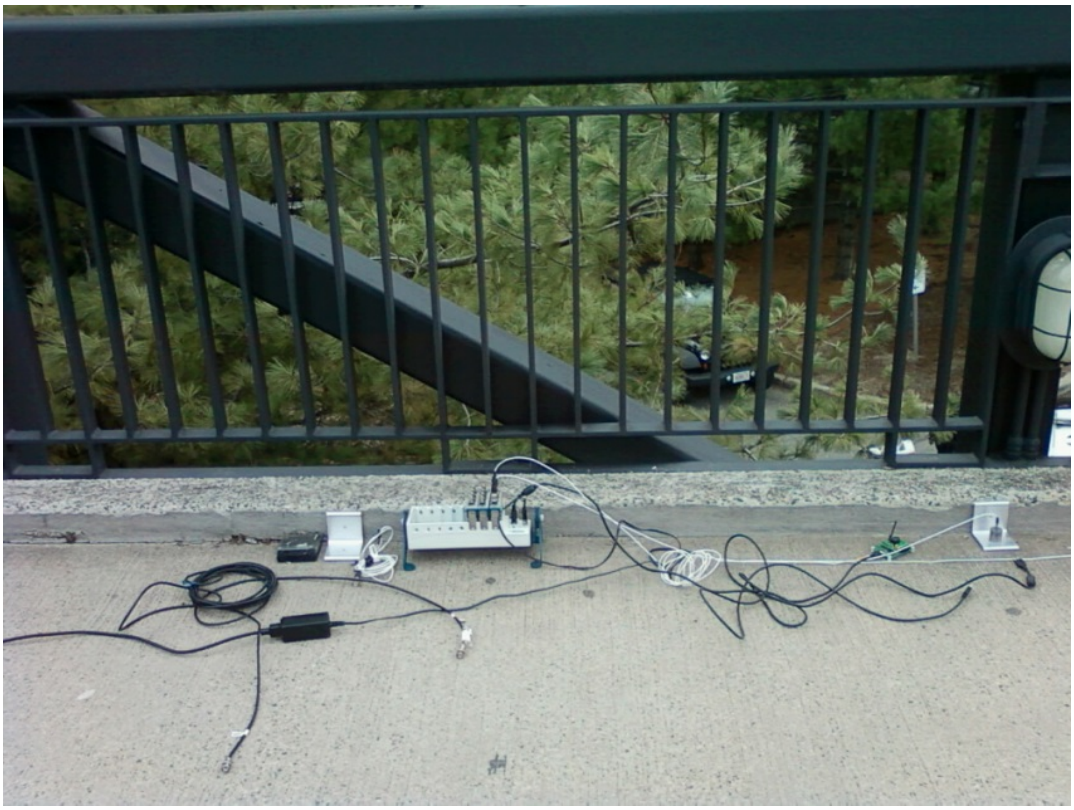

Figure 28: PCB Accelerometers in Test 2 (Right Side of the Bridge)

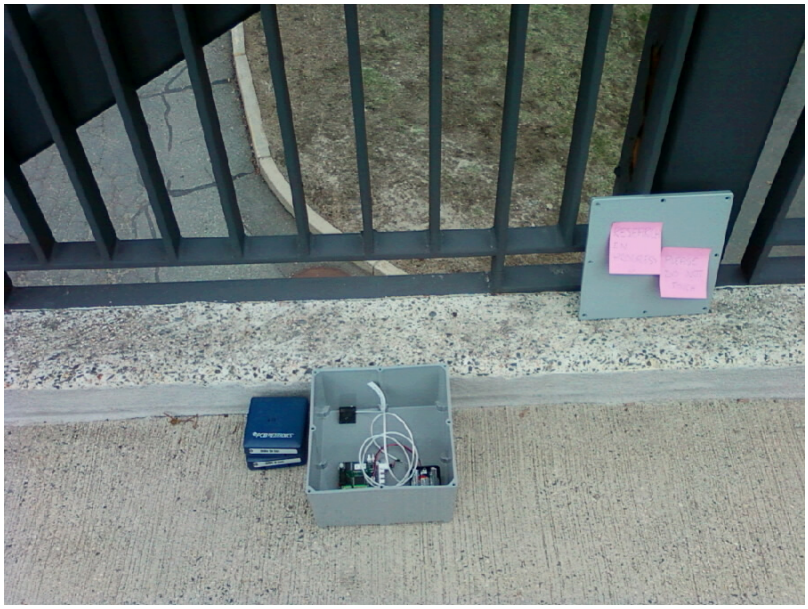

Figure 29: Narada Node in Test 2 (Left Side of the Bridge)

Because I placed the accelerometers in varying locations, I had a difficult time comparing the data, and therefore, I have not displayed the results here. In the next test, I addressed these errors by relocating the sensors.

2.4 Test 3: Narada Node Test Alongside PCB 393B04's with Location Change

Therefore, for Test 3, I relocated all of the sensors to the center of the bridge's width in order to collect more comparable signals. I Here, I tested the sensors next to each other on the Dowling Hall side span. By testing the sensors on the Dowling Hall side span, I could keep the PCB accelerometers closer to each other since the extension cord was limited in length. For this test, I used the following PCB accelerometers:

Table 4: PCB Accelerometers on the Footbridge for Bridge Test 3

PCB 393B04 25398	1055 mV/g
PCB 393B04 25401	1050 mV/g
PCB 393B04 25402	984 mV/g

Figure 30: Setup for Test 3 (Sensors at Center of Bridge)

The same data collection processes applied here as in Test 2. Below are the signals and FFT plots of Trial 1 from this test, during which I ran data collection for about 60 seconds. Figure 33 shows a plot of the FFT for the entire signal collected. The subsequent FFT plots show the FFT for the signal in varying increments. Figure 36 shows the best comparison between the

PCB and Narada FFT plots. Each of the FFT plots for the varying increments display the first natural frequency very clearly, but do not show the succeeding natural frequencies as distinctly. I also ran three trials lasting 5 minutes. For these trials, the Narada node displayed unusual signals; the signals showed a large spike in magnitude every 40 seconds for the duration of the test beginning at t = 35 seconds and a small spike in magnitude every 40 seconds beginning at t = 55 seconds. Because of the errors in these three trials, I have not displayed the results here.

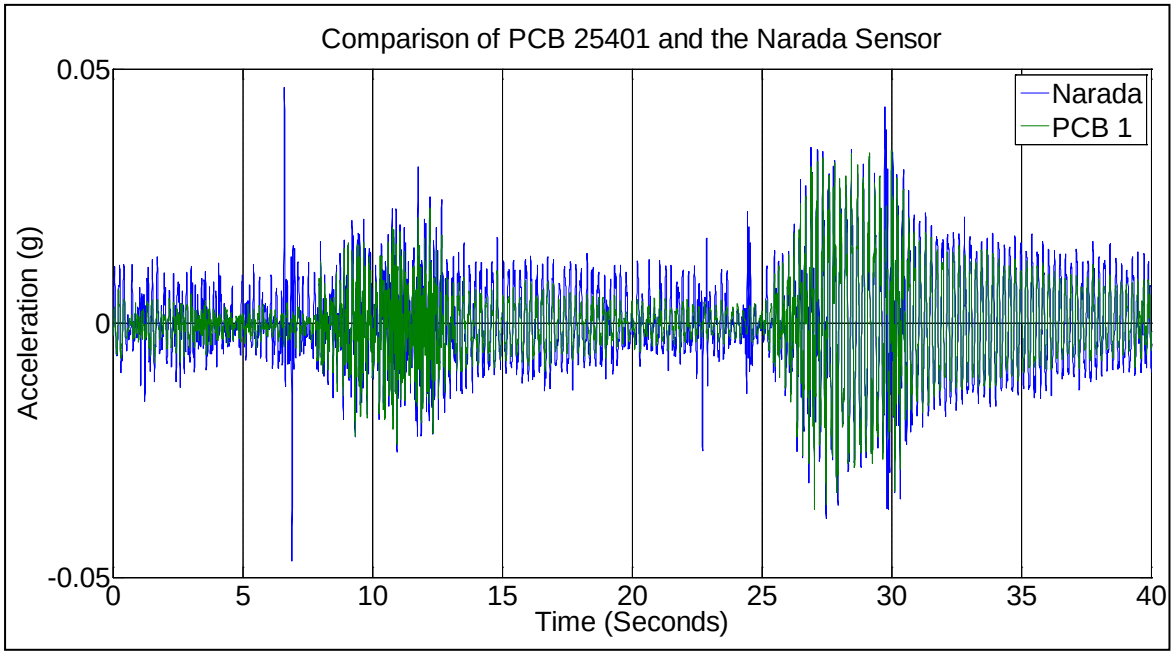

Figure 31: Test 3, Trial 1

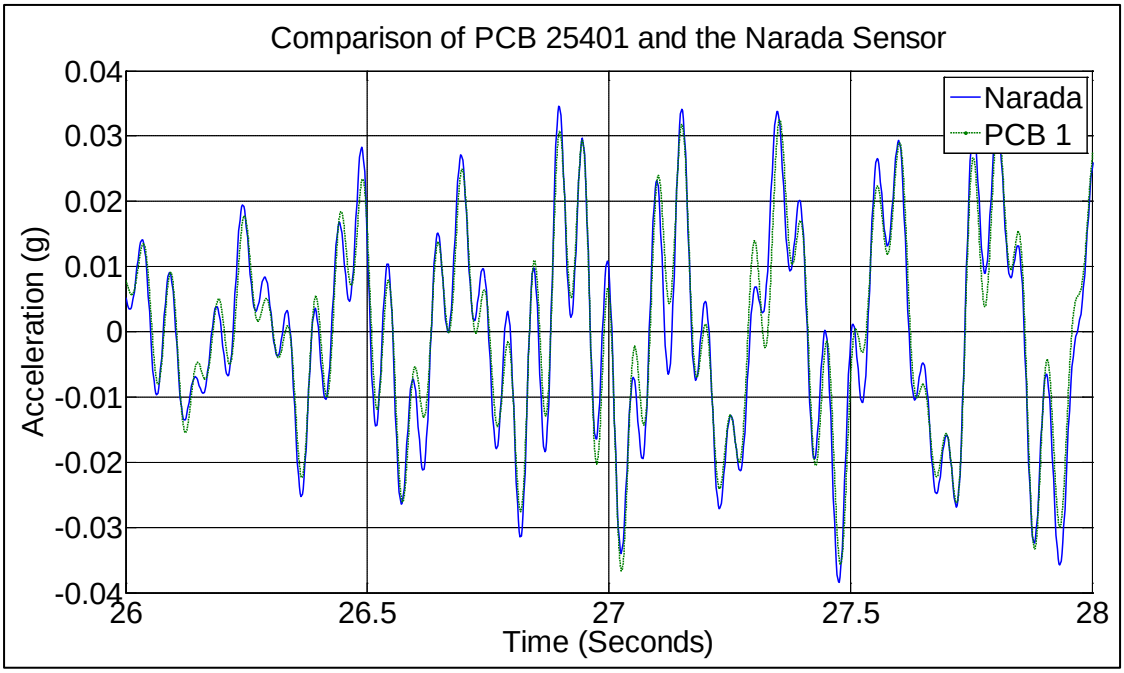

Figure 32: Close-up of Figure 31

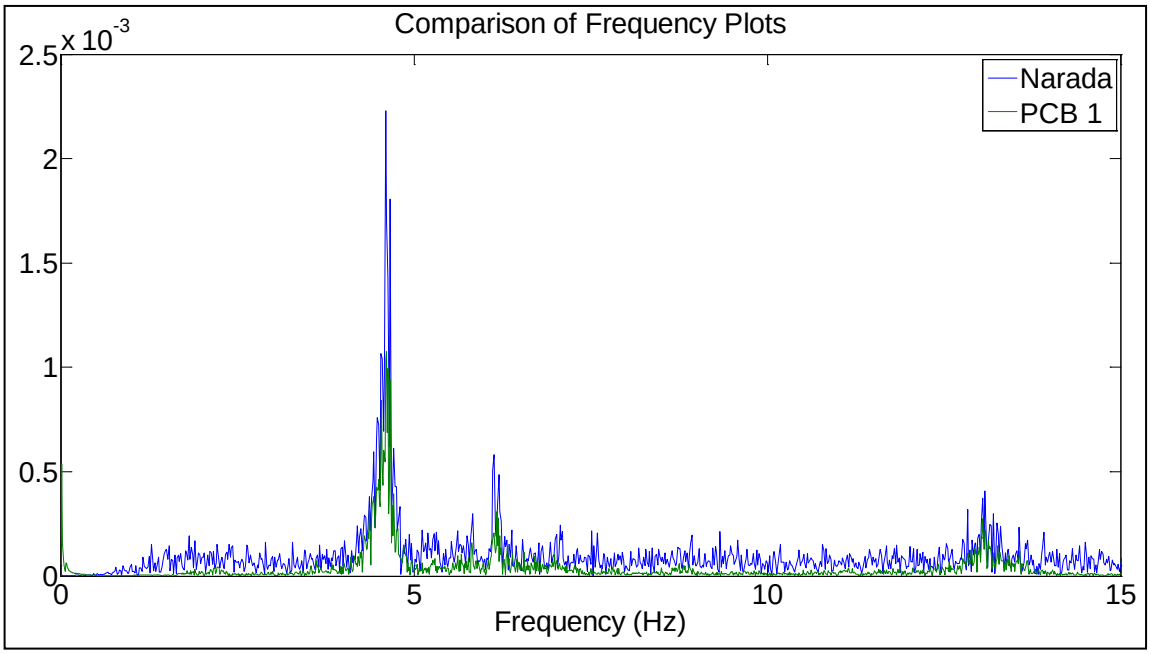

Figure 33: Test 3, Trial 1

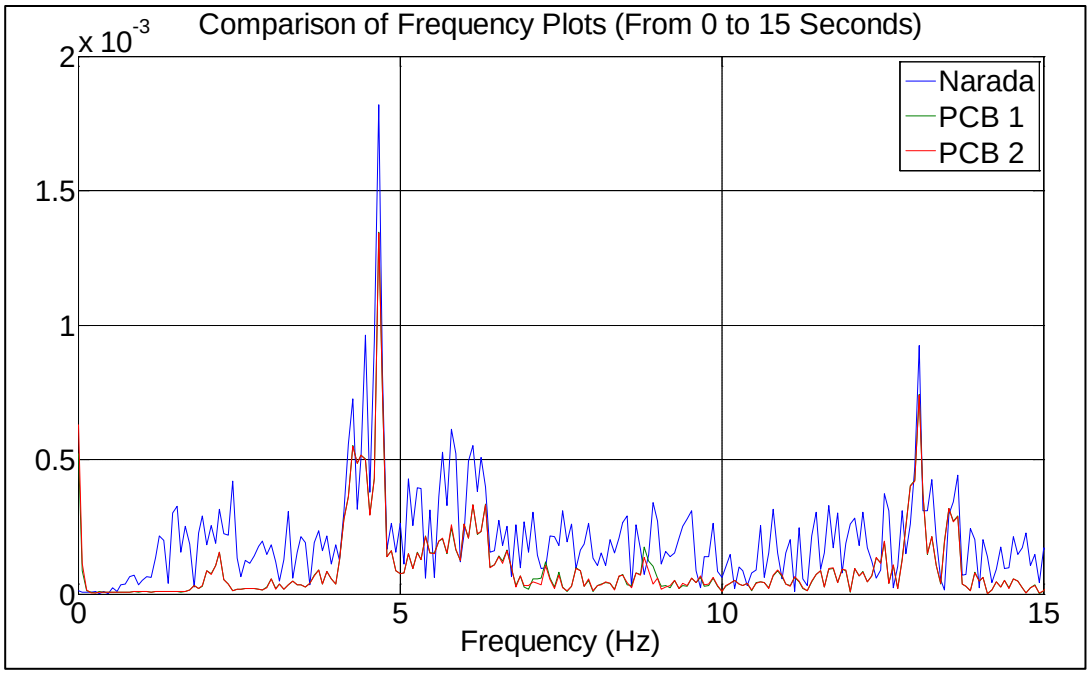

Figure 34: Test 3, Trial 1 FFT Comparison 0-15 Seconds

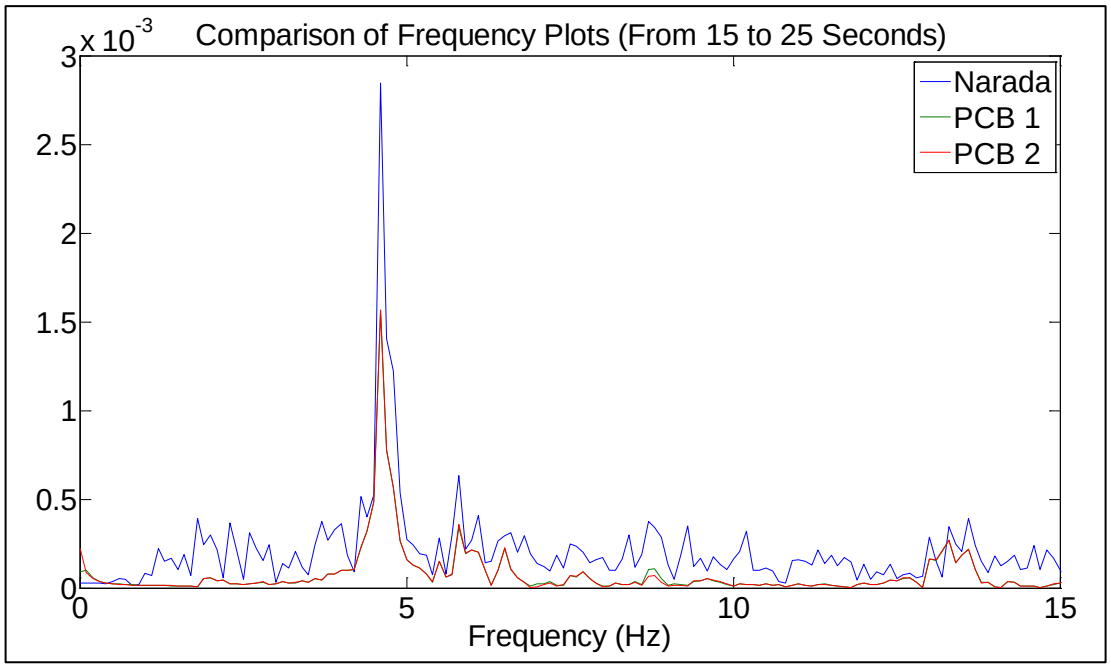

Figure 35: Test 3, Trial 1 FFT Comparison 15-25 Seconds

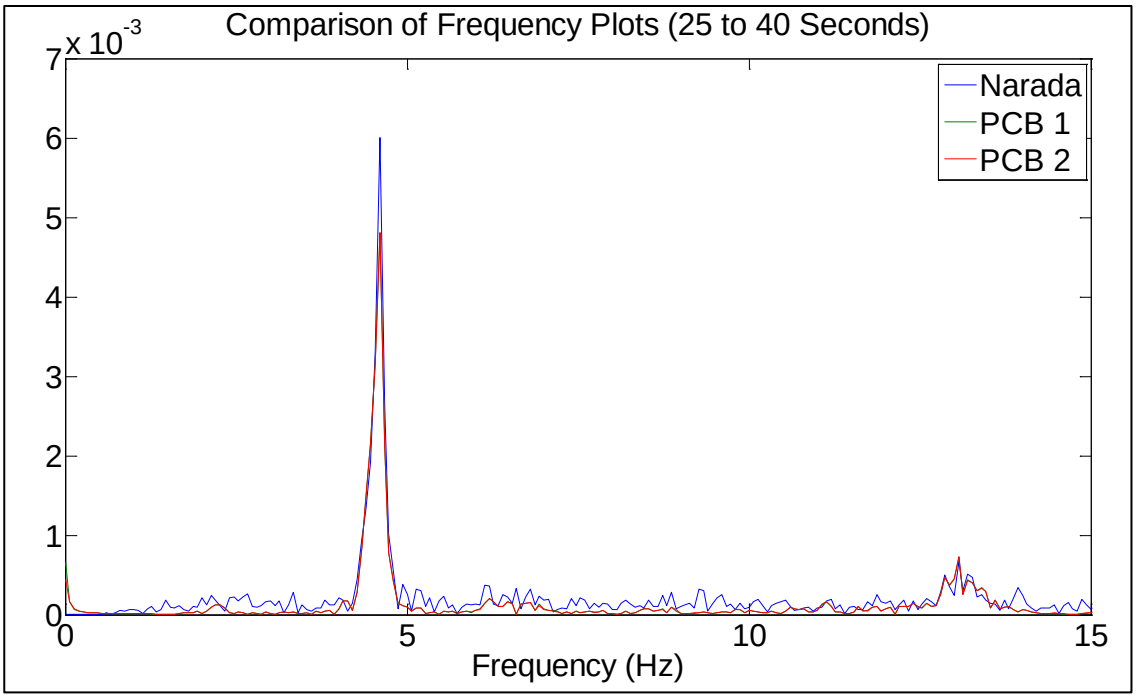

Figure 36: Test 3, Trial 1 FFT Comparison 25-40 Seconds

2.5 Test 4: Narada Node Test Alongside PCB 393B04's with 4-Minute Trials

During Test 4, I re-ran the extended time trials due to the unusual signals from Test 3. In attempts to alleviate any possible errors, I checked that the Silicon Designs 2012-002 was still properly connected to the Narada WSU. I also ensured the Base Station was completely plugged into the laptop. I also adjusted the settings of the sensor before bringing the equipment back out to the bridge. I decided to reduce the sampling rate to 256 Hz and test length to 4 minutes. After changing these settings, the sensor was working normally in Anderson 206A, so I proceeded to test 4.

For the PCB accelerometers, the same data collection process applied. The sensors again sat on the Dowling Hall side span of the bridge and in the middle of the bridge's width.

Table 5: PCB Accelerometers on the Footbridge for Bridge Test 4

PCB 393B04 25401	1050 mV/g
PCB 393B04 25402	984 mV/g

In total, I ran three trials for this final test. The results from Trial 1 are displayed below. Figure 39 shows the FFT plot for the entire signal, while Figure 40 shows the FFT plot for a 20-second increment of the signal.

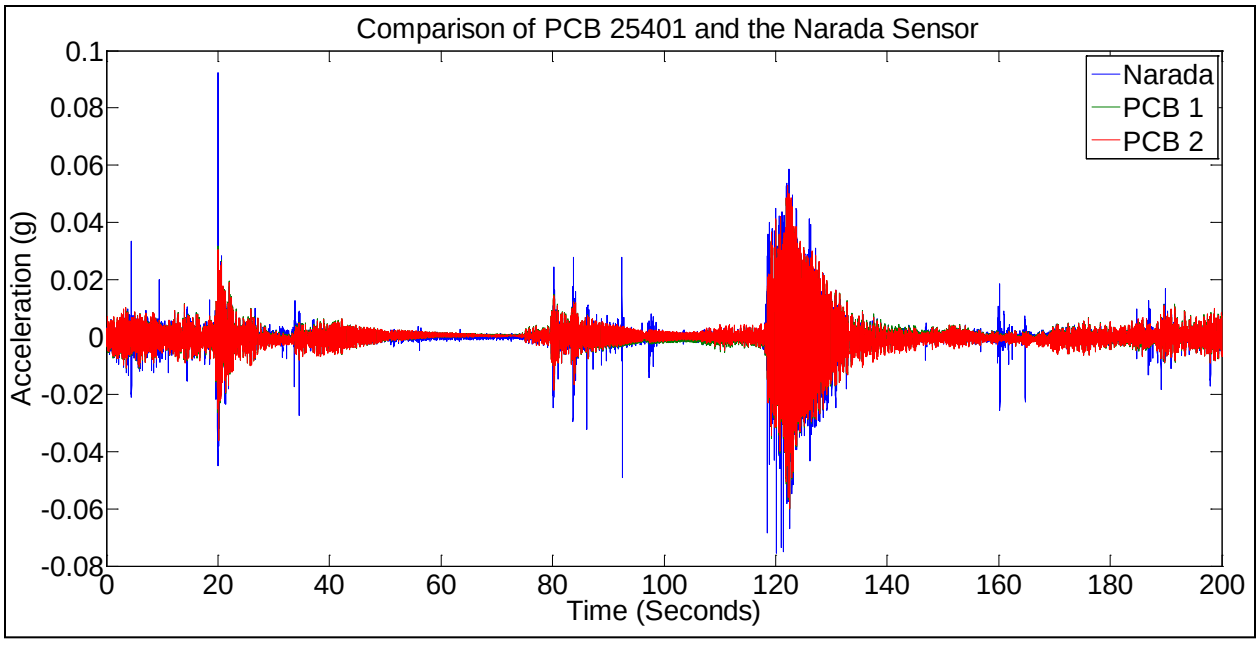

Figure 37: Test 4, Trial 1

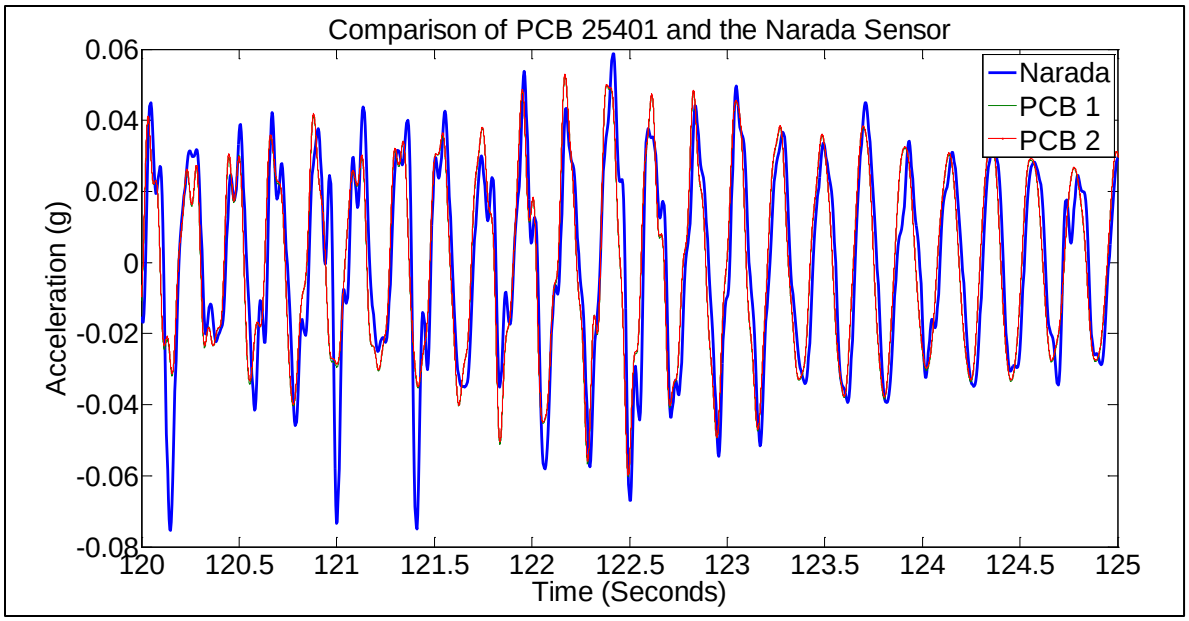

Figure 38: Close-up of Figure 37

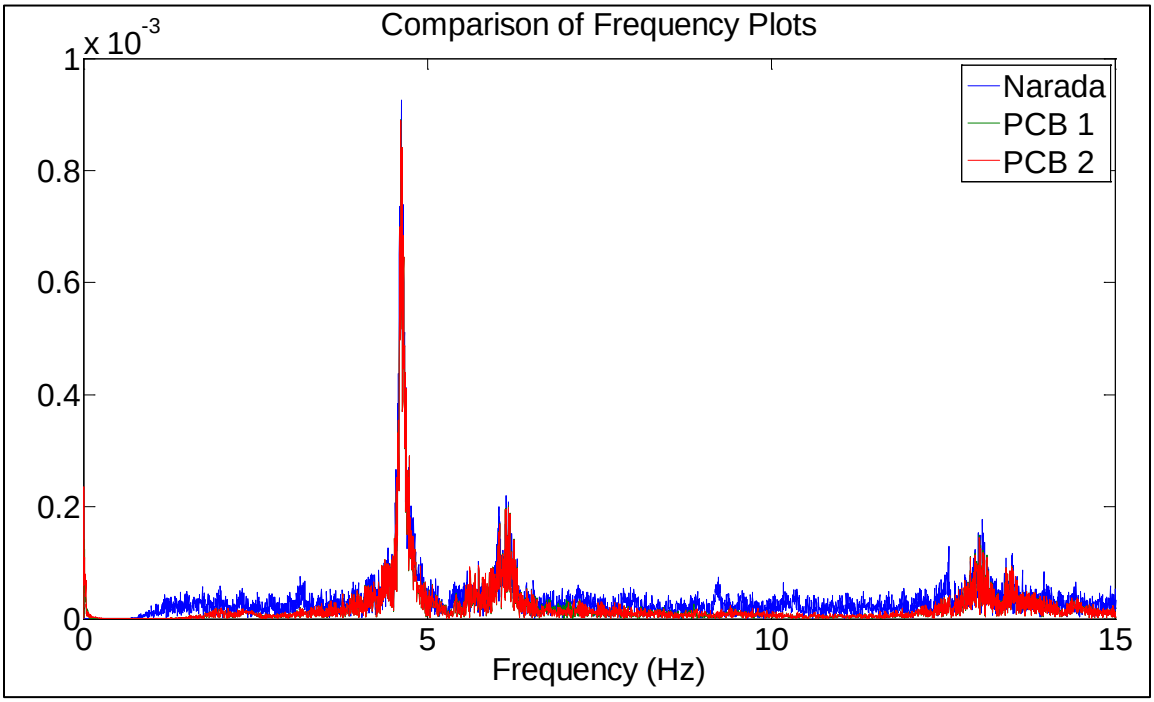

Figure 39: Test 4, Trial 1

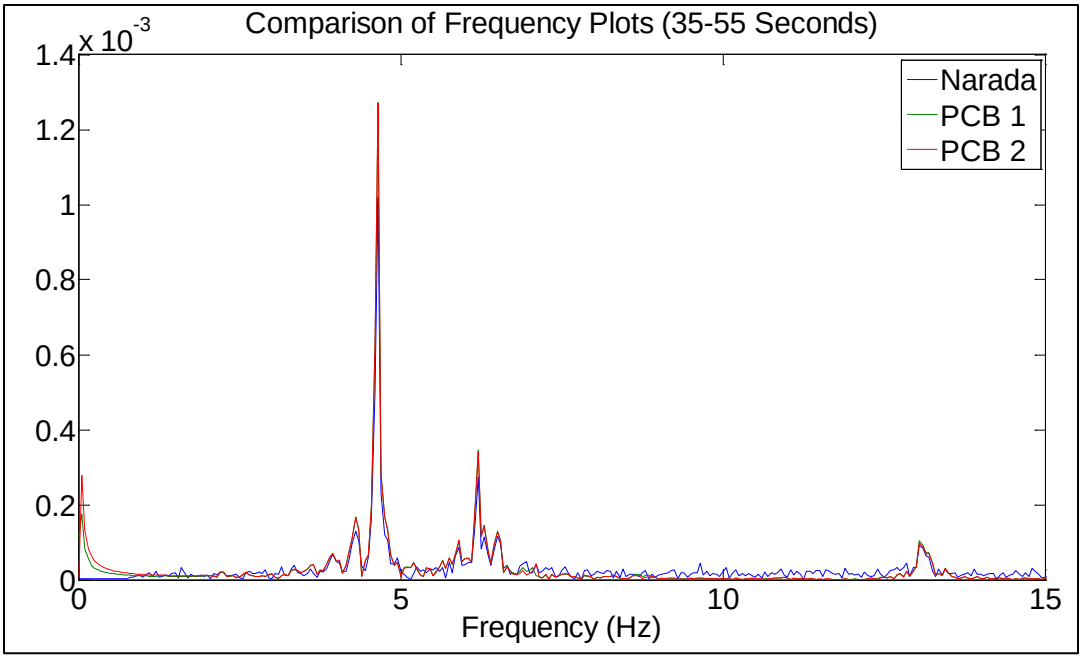

Figure 40: Test 4, Trial 1 FFT Comparison 35-55 Seconds

The first two natural frequencies estimated by the Narada sensor and their errors for Test 4 are displayed here below:

Table 6: Predicted Error in Natural Frequency Estimations

Test 4: Vibration Mode	Natural Frequency (Hz)	Percent Error
1 (Error from Moser)	4.62	1.28%
2 (Error from Moser)	6.17	3.02%
1 (Between Narada and PCB)	4.621 (Narada); 4.612 (PCB)	0.195%
2 (Between Narada and PCB)	6.2 (Narada); 6.2 (PCB)	0.0%

3.0 FURTHER DISCUSSION OF RESULTS

3.1 Discussion of Collected Signals from the Narada Sensor Node

Overall, the signals collected by the Narada sensor (Narada WSU and Silicon Designs 2012-002) decently matched the signals from the PCB accelerometers. With the cDAQ system, the PCB accelerometers are required to have a sampling frequency of at least 1652 Hz, and they have a higher sensitivity than the Silicon Designs accelerometer. When filtered, the signals from the Narada node have similar magnitudes to the signals from the PCB accelerometers. However, the signals from the Narada node also pick up more noise and at times, have unexpected spikes in magnitude. The Narada node also received unusual signals from tests that ran up to 5-minutes using the 512 Hz sampling frequency from 60-second tests. A sampling frequency of 256 Hz and a test length of 4-minutes fixed this problem for the Narada sensor. The unexpected signals could have been due to the non-standard sampling rate. The Narada WSU typically expects a sampling rate that divides evenly into 1,000,000 [5]. The signal spikes occurred before the completion of each polling cycle, and therefore, appear to be a problem with the data acquisition settings.

During the bridge tests I conducted, inconsistent loading on the bridge could have affected the comparison of results. In particular, during Test 3, the bridge experienced an unusual amount of pedestrian traffic because there was an unexpected number of visitors to admissions on that day. With increased traffic and therefore vibrations, the difference between test jumps and other movement was difficult to distinguish.

3.2 Discussion of Frequency Plots

The frequency plots comparing the PCB 393B04 accelerometers and the Narada sensor showed that the accelerometers all picked up similar natural frequencies from the bridge. The main discrepancy between plots was in the magnitude of the FFT value. The PCB accelerometers always had much higher FFT values than the Narada sensor.

In Test 1, six natural frequencies are clearly visible for Trials 1, 4, and 5. For Tests 3 however, natural frequencies 3 and 4 are much less distinguishable for both the plots from the Narada sensor and the plots from the PCB accelerometers. This is most likely due to the location of the sensors, which are close to the modal nodes.

3.3 Discussion of Errors in Natural Frequency

As previously discussed in section 1.4, the Dowling Hall Footbridge has the following natural frequencies [8]:

Table 7: Natural Frequencies of the Dowling Hall Footbridge

Vibration Mode	Natural Frequency (Hz)
1	4.68
2	5.99
3	7.16
4	8.93
5	13.18

6	13.71

Using the same error analysis equations I used in the shaker test, I calculated the errors between the test results of the Narada sensor from the bridge and the tests previously done on the bridge for the first and second natural frequencies. (Appendix A) The errors I calculated are displayed below, using an average of the natural frequencies from each trial:

Table 8: Percent Errors in Natural Frequencies Measured by the Narada Node

Bridge Test	Vibration Mode	Average Natural Frequency (Hz)	Percent Error
1	1	4.6	1.3%
1	2	6.1	1.7%
3 (60-sec Trial)	1	4.6	1.7%
3 (60-sec Trial)	2	6.1	2.4%
4	1	4.6	1.3%
4	2	6.2	3.0%

The natural frequencies found in this project match the natural frequencies found in Moser's thesis well, but in general, these are not completely accurate representations of error for the Narada node. Because the bridge's natural frequencies vary with environmental changes, the bridge's natural frequencies measured in this project are not necessarily the same as they were during the tests done in 2009 [9, 10]. The low error between natural frequencies measured by the

PCB accelerometers and Narada node in this project are a better indication that the Narada node is capable of picking up the bridge's natural frequencies (see Table 6).

4.0 CONCLUSIONS

4.1 Summary

In conclusion, my tests of the Narada sensor for the Cataldo Research Scholarship and for my Senior Thesis confirmed that the Narada WSU and Silicon Designs 2012-002 together are suitable for a wireless sensor network for the Dowling Hall Footbridge. The entire sensor collected signals comparable to the signals that the PCB 393B04 sensors collected. Furthermore, through a Fast Fourier Transform analysis, the Narada WSU's signals displayed natural frequencies within 1% - 3% error of the first two natural frequencies previously determined by Peter Moser in his Master's thesis and less than 1% error when compared only to the PCB accelerometers' FFT plots from this research project. [8]

The main challenges I encountered when using the Narada WSU occurred during setup. At first, I had connection issues between the Narada WSU and the 2012-002 because the pins of the WSU were not in full contact with the wires of the 2012-002. Also, in bridge test 3, the signals the WSU collected experienced unexplained spikes every 40 seconds. I regard this as a setup challenge because adjusting the DAQ settings resolved the issue. By reducing the time length of the test and the sampling frequency, the Narada WSU collected signals normally. Therefore, the Narada WSU is potentially problematic in SHM systems that require high sampling frequencies and continuous monitoring at the same time.

4.2 Future Work and Recommendations

For future work, the Narada sensor may be an outdated option for a wireless sensing system. Since its start, the Narada sensor has been used in various applications for structural health monitoring on civil structures. The Narada sensor typically uses sampling frequencies from 20-100 Hz, so by increasing the sampling frequency in these tests, the data collection system slowed down. A high sampling frequency for the Narada sensor will cause longer transmission times for data collection, which is not sustainable for continuous monitoring. Furthermore, the Narada node could have experienced errors in longer tests because I used a non-standard sampling rate (512 Hz vs. 500 Hz) for most of the tests in this project.

Civionics will release a new wireless sensing platform this year, called Constellation. This updated platform and data acquisition system will hopefully resolve any outstanding issues from the Narada WSU. Additionally, Professor Yang Wang at the Georgia Institute of Technology recently developed Martlet, a new wireless sensing unit with collaborators from the University of Michigan that has a more powerful microprocessor than the Narada WSU. This would allow the WSU to expedite data collection and possibly allow for more flexible values for sampling frequency or time length. The Martlet has an 80 MHz processor and a hardware floating point unit.

Finally, in regards to implementing any wireless sensing system for structural health monitoring on the Dowling Hall Footbridge, attachment to the bridge will pose another challenge. For this project, the Narada sensor was located on top of the bridge, but this will not be practical for an entire array as it would impede pedestrian traffic. The PVC fitting is suitable

for protection from weather, and there are a few options for attachment. The fittings could be epoxied to the bottom of the bridge or attached through another mounting mechanism.

Future research in wireless sensing on the Dowling Hall Footbridge will help gain a better understanding of the challenges such a system faces. As in this project, the challenges were not just battery power, but also in accurately comparing the data from wireless sensors to wired sensors. Finding ways to make these comparisons accurately is important to attaining a comprehensive evaluation of a structure and its structural health monitoring system.

REFERENCES

[1] "Model 2012-002 Datasheet." http://www.silicondesigns.com/pdfs/2012.pdf .

[2] "TG Series Datasheet." http://www.memsic.com/userfiles/files/Datasheets/Accelerometer-Datasheets/TG_Series_Datasheet.pdf .

[3] American Society of Civil Engineers. (2013). "Bridges: Conditions and Capacity." http://www.infrastructurereportcard.org/a/#p/bridges/conditions-and-capacity (2014, 02/01, 2014).

[4] Bordoni, F., and D'Amico, A. (1990). "Noise in Sensors." (Sensors and Actuators, A21-A23), 17.

[5] Civionics Support. "Narada Wireless Sensing System (Version 3.0): Operating Instructions (Windows)."

[6] Farrar, C. R., and Worden, K. (2006). "An Introduction to Structural Health Monitoring." (Philosophical Transactions of the Royal Society A), 303.

[7] Lynch, J.P., and Loh, K.J. (2006). “A Summary Review of Wireless Sensors and Sensor Networks for Structural Health Monitoring.” The Shock and Vibration Digest, 38(2), 91-128.

[8] Moser, P. (2010). "Continuous Monitoring of the Dowling Hall Footbridge". MS in Civil Engineering. Tufts University, Medford, MA.

[9] Moser, P., and Moaveni, B. (2010). “Environmental effects on the identified natural frequencies of the Dowling Hall Footbridge.” Mechanical Systems and Signal Processing, 25(7), 2336-2357.

[10] Sohn, H., Farrar, C.R., Hemez, F.M., Shunk, D.D., Stinemates, D.W., and Nadler, B.R. (2003). A review of structural health monitoring literature: 1996-2001. Technical Report , Los Alamos National Laboratory; LA-13976-MS, Los Alamos, New Mexico, USA.

[11] The Colbert Report. (2013). "Tiny Triumphs - Infrastructure and River Pollution." http://thecolbertreport.cc.com/videos/06tavh/tiny-triumphs---infrastructure---river-pollution (02/01, 2014).

Appendix A

Code for Shaker Tests

```
clear all
clc
close all

% Data and Time/Frequency vectors
num = xlsread('0329_folder100');

input = dlmread('input_scaled.txt'); % 50 hz
tinput = 0:(1/50):(length(input)-1)*(1/50);

fs = 512;
[N,n1] = size(num);
dt = 1/fs;
t = 0:dt:(N-1)*dt;
df = 1/t(end);
f = 0:df:(N-1)*df;

g = detrend((num*5/65535 - 2.5)/1, 'constant');

yuan = '0329_trial5_yuan';
cdaq = '0329_trial5_cDAQ';

pcb1 = detrend(xlsread(yuan, '', 'A1:A16384'), 'constant')/-1.059;
pcb2 = detrend(xlsread(yuan, '', 'B1:B16384'), 'constant')/-1.055;

N1 = length(pcb1);
t1 = 0:dt:(N1-1)*dt;
df1 = 1/t1(end);
f1 = 0:df1:(N1-1)*df1;

pcb3 = detrend(xlsread(cdaq, '', 'A1:A278528'), 'constant')/1.05;
pcb4 = detrend(xlsread(cdaq, '', 'B1:B278528'), 'constant')/0.984;
bnk = detrend(xlsread(cdaq, '', 'C1:C278528'), 'constant')/0.349;

fs2 = 2048;
N2 = length(pcb3);
t2 = 0:1/fs2:(N2-1)/fs2;
df2 = 1/t2(end);
f2 = 0:df2:(N2-1)*df2;

N3 = length(bnk);
t3 = 0:1/fs2:(N3-1)/fs2;
df3 = 1/t3(end);
f3 = 0:df3:(N3-1)*df3;

figure(1)
plot(t,g, t1,pcb1,'r', t1, pcb2,'g', t2,pcb3, 'c', t2, pcb4, 'k', t3, bnk,
'm'); legend('g','pcb1', 'pcb2', 'pcb3', 'pcb4', 'bnk')
xlim([0 40])

fn1 = fs/2;
fn3 = fs2/2;
```

```
fcutoff = 20; fcutin  = 0.5;

b1 = fir1(2048, [fcutin/fn1 fcutoff/fn1], 'bandpass');
[h1,ff1] = freqz(b1,1,N,'whole',fs);

figure(2)
subplot(1,2,1)
plot(ff1,abs(h1))
xlim([0 30])

g_f = filter(b1,1,g);
g_f = detrend([g_f(1025:end);zeros(1024,1)],'constant'); % correction for
filter delay

pcb1_f = filter(b1,1,pcb1);
pcb1_f = detrend([pcb1_f(1025:end);zeros(1024,1)],'constant'); % correction
for filter delay

pcb2_f = filter(b1,1,pcb2);
pcb2_f = detrend([pcb2_f(1025:end);zeros(1024,1)],'constant'); % correction
for filter delay

b3 = fir1(2048,[fcutin/fn3 fcutoff/fn3],'bandpass');
[h3,ff3] = freqz(b3,1,N3,'whole',fs2);

figure(2)
subplot(1,2,2)
plot(ff3,abs(h3))
xlim([0 30])

pcb3_f = filter(b3,1,pcb3);
pcb3_f = detrend([pcb3_f(2049:end);zeros(2048,1)],'constant'); % correction
for filter delay

pcb4_f = filter(b3,1,pcb4);
pcb4_f = detrend([pcb4_f(2049:end);zeros(2048,1)],'constant'); % correction
for filter delay

bnk_f = filter(b3,1,bnk);
bnk_f = detrend([bnk_f(2049:end);zeros(2048,1)],'constant'); % correction for
filter delay

figure(3)
subplot(2,1,1)
plot(t,g_f, t1,pcb1_f,'r', t1, pcb2_f,'g', t2,pcb3_f, 'c', t2, pcb4_f, 'k',
t3, bnk_f, 'm'); legend('g','pcb1', 'pcb2', 'pcb3', 'pcb4', 'bnk')
xlim([0 40]);

% Time Synchronization

[ii1,iii1] = max(g_f(13.8*fs:13.9*fs)); iii1 = iii1 + round(3.8*fs);
[ii2,iii2] = max(pcb1_f(10.8*fs:10.9*fs));  iii2 = iii2 + round(0.8*fs);
[ii3,iii3] = max(pcb3_f(17.8*fs2:17.9*fs2));  iii3 = iii3 + round(7.8*fs2);
```

```
[ii4,iii4] = max(bnk_f(17.8*fs2:17.9*fs2));  iii4 = iii4 + round(7.8*fs2);

ii1 = 1; ii2 = 1; ii3 = 1; ii4 = 1;

subplot(2,1,2)
plot(t(iii1:end)-t(iii1),g_f(iii1:end)/ii1, t1(iii2:end)-t1(iii2),
pcb1_f(iii2:end)/ii2, t2(iii3:end)-t2(iii3),pcb3_f(iii3:end)/ii3,
t3(iii4:end)-t3(iii4),bnk_f(iii4:end)/ii4)
legend('g','pcb1', 'pcb3', 'bnk')
xlim([0 40]);

% FFT
figure(4)
plot(f,abs(fft(g_f))/length(f), f1, abs(fft(pcb1_f))/length(f1), f2,
abs(fft(pcb3_f))/length(f2), f3, abs(fft(bnk))/length(f3));
legend('g','pcb1','pcb3', 'bnk')
xlim([0 15])


% Error for 20-30 seconds

start21 = (iii1+10220); last21 = (iii1+14900);
start22 = (iii2+10220); last22 = (iii2+14900);
start23 = (iii3+40880); last23 = (iii3+59600);
start24 = (iii4+40880); last24 = (iii4+59600);

x1 = abs(g_f(start21:last21)/ii1);
x2 = abs(pcb1_f(start22:last22)/ii2);
x3 = abs(pcb3_f(start23:last23)/ii3);
x4 = abs(bnk_f(start24:last24)/ii4);

e1 = abs(g_f(start21:last21)/ii1-pcb1_f(start22:last22)/ii2);
e2 = abs(g_f(start21:last21)/ii1-pcb3_f(start23:4:last23)/ii3);
e3 = abs(g_f(start21:last21)/ii1-bnk_f(start24:4:last24)/ii4);
e4 = abs(pcb1_f(start22:last22)/ii2-pcb3_f(start23:4:last23)/ii3);
e5 = abs(pcb3_f(start23:4:last23)/ii3-bnk_f(start24:4:last24)/ii4);

E1 = (e1'*e1)/(x2'*x2)*100
E2 = (e2'*e2)/(x3'*x3)*100
E3 = (e3'*e3)/(x4'*x4)*100
E4 = (e4'*e4)/(x2'*x2)*100;
E5 = (e5'*e5)/(x3'*x3)*100;

% Error for 0-10 seconds

start11 = iii1; last11 = (iii1+5120);
start12 = iii2; last12 = (iii2+5120);
start13 = iii3; last13 = (iii3+20480);
start14 = iii4; last14 = (iii4+20480);

x11 = abs(g_f(start11:last11)/ii1);
x12 = abs(pcb1_f(start12:last12)/ii2);
x13 = abs(pcb3_f(start13:last13)/ii3);
x14 = abs(bnk_f(start14:last14)/ii4);
```

```
e11 = abs(g_f(start11:last11)/ii1-pcb1_f(start12:last12)/ii2);
e12 = abs(g_f(start11:last11)/ii1-pcb3_f(start13:4:last13)/ii3);
e13 = abs(g_f(start11:last11)/ii1-bnk_f(start14:4:last14)/ii4);
e14 = abs(pcb1_f(start12:last12)/ii2-pcb3_f(start13:4:last13)/ii3);
e15 = abs(pcb3_f(start13:4:last13)/ii3-bnk_f(start14:4:last14)/ii4);

E11 = (e11'*e11)/(x12'*x12)*100
E12 = (e12'*e12)/(x13'*x13)*100
E13 = (e13'*e13)/(x14'*x14)*100
E14 = (e14'*e14)/(x12'*x12)*100;
E15 = (e15'*e15)/(x13'*x13)*100;

% Error for 10-20 seconds

start31 = (iii1+5120); last31 = (iii1+10220);
start32 = (iii2+5120); last32 = (iii2+10220);
start33 = (iii3+20480); last33 = (iii3+40880);
start34 = (iii3+20480); last34 = (iii4+40880);

x31 = abs(g_f(start31:last31)/ii1);
x32 = abs(pcb1_f(start32:last32)/ii2);
x33 = abs(pcb3_f(start33:last33)/ii3);
x34 = abs(bnk_f(start34:last34)/ii4);

e31 = abs(g_f(start31:last31)/ii1-pcb1_f(start32:last32)/ii2);
e32 = abs(g_f(start31:last31)/ii1-pcb3_f(start33:4:last33)/ii3);
e33 = abs(g_f(start31:last31)/ii1-bnk_f(start34:4:last34)/ii4);
e34 = abs(pcb1_f(start32:last32)/ii2-pcb3_f(start33:4:last33)/ii3);
e35 = abs(pcb3_f(start33:4:last33)/ii3-bnk_f(start34:4:last34)/ii4);

E31 = (e31'*e31)/(x32'*x32)*100
E32 = (e32'*e32)/(x33'*x33)*100
E33 = (e33'*e33)/(x34'*x34)*100
E34 = (e34'*e34)/(x32'*x32)*100;
E35 = (e35'*e35)/(x33'*x33)*100;
```

Code for Bridge Test 3

```
clear all
clc
close all

num = xlsread('folder121');

fs = 512;
[N,n1] = size(num);
dt = 1/fs;
t = 0:dt:(N-1)*dt;
df = 1/t(end);
f = 0:df:(N-1)*df;

g = detrend((num*5/65535 - 3.5)/1, 'constant');

cdaq = '0414_5';
```

```
pcb = detrend(xlsread(cdaq), 'constant');
pcb1 = pcb(:,1);
pcb2 = pcb(:,2);
pcb3 = pcb(:,3);

N1 = length(pcb1);
fs1 = 2048;
dt1 = 1/fs1;
t1 = 0:dt1:(N1-1)*dt1;
df1 = 1/t1(end);
f1 = 0:df1:(N1-1)*df1;

figure(1)
plot(t,g, t1, pcb1, 'r', t1, pcb2, 'g', t1, pcb3, 'm')
xlim([0 100])

fn1 = fs/2;
fn2 = fs1/2;
fcutoff = 20; fcutin  = 1.0;

b1 = fir1(1024, [fcutin/fn1 fcutoff/fn1], 'bandpass');
[h1,ff1] = freqz(b1,1,N,'whole',fs);

b2 = fir1(2048,[fcutin/fn2 fcutoff/fn2],'bandpass');
[h2,ff2] = freqz(b2,1,N1,'whole',fs1);

figure(2)
subplot(1,2,1)
plot(ff1,abs(h1))
xlim([0 30])
subplot(1,2,2)
plot(ff2,abs(h2))
xlim([0 30])

g_f = filter(b1,1,g);
g_f = detrend([g_f(1025:end);zeros(1024,1)],'constant'); % correction for
filter delay

pcb1_f = filter(b2,1,pcb1);
pcb1_f = detrend([pcb1_f(2049:end);zeros(2048,1)],'constant'); % correction
for filter delay

pcb2_f = filter(b2,1,pcb2);
pcb2_f = detrend([pcb2_f(2049:end);zeros(2048,1)],'constant'); % correction
for filter delay

figure(3)
subplot(2,1,1)
plot(t,g_f, t1, pcb1_f,'r',t1,pcb2_f,'g'); legend('g','pcb1','pcb2');
xlim([0 60]);

[ii1,iii1] = max(g_f(35*fs:38*fs)); iii1 = iii1 + round(5*fs) + 132;
[ii2,iii2] = max(pcb1_f(55*fs1:60*fs1));  iii2 = iii2 + round(25*fs1);
[ii3,iii3] = max(pcb2_f(55*fs1:60*fs1));  iii3 = iii3 + round(25*fs1);
```

```
figure(3)
subplot(2,1,2)
plot(t(iii1:end)-t(iii1),g_f(iii1:end), t1(iii2:end)-t1(iii2),
pcb1_f(iii2:end), t1(iii3:end)-t1(iii3),pcb2_f(iii3:end))
legend('g','pcb1', 'pcb2')
xlim([0 40]);


% FFT
figure(4)
plot(f,abs(fft(g_f)/length(f)), f1,
abs(fft(pcb1_f))/length(f1),f1,abs(fft(pcb2_f))/length(f1));
legend('g','pcb1','pcb2');
xlim([0 15])

fs2 = 512;
N2 = length(g_f((25*fs2+iii1):(40*fs2+iii1)));
dt2 = 1/fs2;
t2 = 0:dt2:(N2-1)*dt2;
df2 = 1/t2(end);
f2 = 0:df2:(N2-1)*df2;

fs3 = 2048;
N3 = length(pcb1_f((25*fs3+iii2):(40*fs3+iii2)));
dt3 = 1/fs3;
t3 = 0:dt3:(N3-1)*dt3;
df3 = 1/t3(end);
f3 = 0:df3:(N3-1)*df3;

figure(5)
plot(f2,abs(fft(g_f((25*fs2+iii1):(40*fs2+iii1)))/length(f2)), f3,
abs(fft(pcb1_f((25*fs3+iii2):(40*fs3+iii2))))/length(f3),f3,abs(fft(pcb2_f((2
5*fs3+iii2):(40*fs3+iii2))))/length(f3)); legend('g','pcb1','pcb2');
xlim([0 15])

fftg = abs(fft(g));
[a b] = max(fftg(1:350))
mode1 = f(b)
pererr = abs(mode1-4.68)/4.68*100
[c d] = max(fftg(350:400))
mode2 = f(d+350)
pererr2 = abs(mode2-5.99)/5.99*100

% Modes identified Moser Thesis, page 90
% 1 4.68 Hz
% 2 5.99
% 3 7.16
% 4 8.93
% 5 13.18
% 6 13.71

delt = -1000:1000;

for i = 1:length(delt)
```

```
    err = g_f(iii1+delt(i)+25*fs:iii1+delt(i)+35*fs) -
pcb1_f(iii2+25*fs1:4:iii2+35*fs1);
    ff(i) = err'*err;
end

figure(6)
plot(delt, ff)

[j1 j2] = min(ff)
j1/(pcb1_f(iii2+25*fs1:4:iii2+35*fs1)'*pcb1_f(iii2+25*fs1:4:iii2+35*fs1))*100
```

Code for Bridge Test 4

```
clear all
clc
close all

num = xlsread('folder141');

fs = 256;
[N,n1] = size(num);
dt = 1/fs;
t = 0:dt:(N-1)*dt;
df = 1/t(end);
f = 0:df:(N-1)*df;

g = detrend((num*5/65535 - 3.5)/1, 'constant');

cdaq = '42214_trial1';
pcb = detrend(xlsread(cdaq), 'constant');
pcb1 = pcb(:,1);
pcb2 = pcb(:,2);

N1 = length(pcb1);
fs1 = 2048;
dt1 = 1/fs1;
t1 = 0:dt1:(N1-1)*dt1;
df1 = 1/t1(end);
f1 = 0:df1:(N1-1)*df1;

figure(1)
plot(t,g, t1, pcb1, 'r', t1, pcb2, 'g')
xlim([0 100])

fn1 = fs/2;
fn2 = fs1/2;
fcutoff = 20; fcutin  = 1.0;

b1 = fir1(1024, [fcutin/fn1 fcutoff/fn1], 'bandpass');
[h1,ff1] = freqz(b1,1,N,'whole',fs);

b2 = fir1(2048,[fcutin/fn2 fcutoff/fn2],'bandpass');
[h2,ff2] = freqz(b2,1,N1,'whole',fs1);
```

```
figure(2)
subplot(1,2,1)
plot(ff1,abs(h1))
xlim([0 30])
subplot(1,2,2)
plot(ff2,abs(h2))
xlim([0 30])

g_f = filter(b1,1,g);
g_f = detrend([g_f(1025:end);zeros(1024,1)],'constant'); % correction for
filter delay

pcb1_f = filter(b2,1,pcb1);
pcb1_f = detrend([pcb1_f(2049:end);zeros(2048,1)],'constant'); % correction
for filter delay

pcb2_f = filter(b2,1,pcb2);
pcb2_f = detrend([pcb2_f(2049:end);zeros(2048,1)],'constant'); % correction
for filter delay

figure(3)
subplot(2,1,1)
plot(t,g_f, t1, pcb1_f,'r',t1,pcb2_f,'g'); legend('g','pcb1','pcb2');
xlim([0 300]);

[ii1,iii1] = max(g_f(28*fs:35*fs)); iii1 = iii1 + round(8*fs);
[ii2,iii2] = max(pcb1_f(40*fs1:45*fs1));  iii2 = iii2 + round(20*fs1);
[ii3,iii3] = max(pcb2_f(40*fs1:45*fs1));  iii3 = iii3 + round(20*fs1);

figure(3)
subplot(2,1,2)
plot(t(iii1:end)-t(iii1),g_f(iii1:end), t1(iii2:end)-t1(iii2),
pcb1_f(iii2:end), t1(iii3:end)-t1(iii3),pcb2_f(iii3:end))
legend('g','pcb1', 'pcb2')
xlim([0 200]);


% FFT
figure(4)
plot(f,abs(fft(g_f)/length(f)), f1,
abs(fft(pcb1_f))/length(f1),f1,abs(fft(pcb2_f))/length(f1));
legend('g','pcb1','pcb2');
xlim([0 15])

fs2 = 256;
N2 = length(g_f((35*fs2+iii1):(55*fs2+iii1)));
dt2 = 1/fs2;
t2 = 0:dt2:(N2-1)*dt2;
df2 = 1/t2(end);
f2 = 0:df2:(N2-1)*df2;

fs3 = 2048;
N3 = length(pcb1_f((35*fs3+iii2):(55*fs3+iii2)));
dt3 = 1/fs3;
t3 = 0:dt3:(N3-1)*dt3;
```

```
df3 = 1/t3(end);
f3 = 0:df3:(N3-1)*df3;

figure(5)
plot(f2,abs(fft(g_f((35*fs2+iii1):(55*fs2+iii1)))/length(f2)), f3,
abs(fft(pcb1_f((35*fs3+iii2):(55*fs3+iii2)))/length(f3)),f3,abs(fft(pcb2_f((3
5*fs3+iii2):(55*fs3+iii2)))/length(f3))); legend('g','pcb1','pcb2');
xlim([0 15])

fftg = abs(fft(g));
[a b] = max(fftg(1:2000))
mode1 = f(b)
pererr = abs(mode1-4.68)/4.68*100
[c d] = max(fftg(2000:30000))
mode2 = f(d+2000)
pererr2 = abs(mode2-5.99)/5.99*100

% Modes identified Moser Thesis, page 90
% 1 4.68 Hz
% 2 5.99
% 3 7.16
% 4 8.93
% 5 13.18
% 6 13.71
```